

**Dissertation**

**Influence of the microenvironment and the role of  
cytokines in chronic thromboembolic pulmonary  
hypertension (CTEPH)**

submitted by

**Mag.rer.nat.**

**Diana ZABINI**

for the Academic Degree of

**Doctor of Philosophy (PhD)**

at the

**Medical University of Graz**

**Department of Anaesthesiology and Intensive Care Medicine**

under the Supervision of

**Prof. Dr. Andrea OLSCHESKI**

**2013**

## **Statutory Declaration**

I hereby declare that this dissertation is my own original work and that I have fully acknowledged by name all of those individuals and organisations that have contributed to the research for this dissertation. Due acknowledgement has been made in the text to all other material used. Throughout this dissertation and in all related publications I followed the guidelines of “Good Scientific Practice”.

Date 12.02.2013

# Table of Contents

<b>Abbreviations and Definitions</b>	4
<b>Abstract in German</b>	5
<b>Abstract in English</b>	7
<b>Introduction</b>	
<i>Chronic thromboembolic pulmonary hypertension (CTEPH)</i>	8
<i>Misguided thrombus resolution</i>	9
<i>Pulmonary thromboendarterectomy (PEA)</i>	11
<i>Vascular endothelial cells</i>	13
<b>Aims</b>	17
<b>Material and Methods</b>	
<i>Isolation of primary human endothelial cells from PEA material</i>	18
<i>Isolation of adventitial fibroblasts from donor lungs</i>	18
<i>Immunohistochemistry</i>	19
<i>Flow-cytometric analysis</i>	19
<i>ELISA</i>	20
<i>RNA-isolation and PCR</i>	20
<i>Proliferation</i>	21
<i>Vessel formation assay</i>	21
<i>Wound healing</i>	22
<i>Permeability measurement with fluorescently labelled dextran</i>	22
<i>Live cell Ca<sup>2+</sup> imaging</i>	22
<i>Chemotaxis assay/Transwell migration</i>	24
<i>Statistical analysis</i>	24
<i>Primers, Antibodies, Substances</i>	24
<b>Flow chart of work sequence</b>	26
<b>Results</b>	
<b>Part 1</b>	
<i>Characteristic parameters of CTEPH patient population</i>	28
<i>Characteristic appearance of PEA surgical material of CTEPH patients</i>	28
<i>Vessels are present in PEA surgical material of CTEPH patients</i>	31

<b>Part 2</b>	
<i>Isolation and characterization of CTEPH-human endothelial cells</i>	32
<b>Part 3</b>	
<i>Angiostatic factors present in the PEA tissue influence calcium homeostasis</i>	38
<i>Angiostatic factors from the PEA tissue lead to endothelial dysfunction</i>	45
<b>Part 4</b>	
<i>Presence of inflammatory factors in CTEPH-tissue</i>	50
<b>Part 5</b>	
<i>Level of inflammatory factors in CTEPH serum</i>	57
<i>Fibroblast are present in the PEA tissue</i>	59
<b>Discussion</b>	62
<b>References</b>	71
<b>Acknowledgement</b>	81

## Abbreviations and Definitions

CI	Cardiac Index
CO	Cardiac Output
CTEPH	Chronic Thromboembolic Pulmonary Hypertension
CTEPH-hEC	Chronic Thromboembolic Pulmonary Hypertension-human Endothelial Cell
CTO	Chronic Total Occlusion
3D-MRA	3 Dimensional Magnetic Resonance Angiogram
EC	Endothelial Cell
ECM	Extracellular matrix
ELISA	Enzyme-linked Immunosorbent Assay
FACS	Fluorescent-activated Cell Sorting
gp	Blood Glycoprotein
HMVEC	Human Microvascular Endothelial Cell
HUVEC	Human Umbilical Vein Endothelial Cell
ICC	Immune cytochemistry
IFN- $\gamma$	Interferon Gamma
IL6	Interleukin 6
IL8	Interleukin 8
IP-10	Interferon Gamma-induced Protein 10
LOX	Lysyl oxidase like
MCP-1	Monocyte Chemoattractant Protein-1
MIG	Monokine induced by Interferon- $\gamma$
MIP1 $\alpha$	Macrophage Inflammatory Protein 1 alpha
MMP	Matrix Metalloproteinase
mPAP	Mean Pulmonary Artery Pressure
NO	Nitric Oxide
NYHA	New York Heart Association
PAEC	Pulmonary Artery Endothelial Cells
PAI-1	Plasminogen-Activator Inhibitor
PASMC	Pulmonary Artery Smooth Muscle Cells
PEA	Pulmonary Endarterectomy
PF4	Platelet Factor 4
PGI <sub>2</sub>	Prostacyclin
PVR	Pulmonary Vascular Resistance
ROC	Receptor Operated Channels
RT-PCR	Reverse Transcriptase Polymerase Chain Reaction
SER	Sarco-Endoplasmatic Reticulum
SERCA	Sarco/Endoplasmic Reticulum Calcium ATPase
sm $\alpha$ -Actin	Smooth Muscle alpha-Actin
SMC	Smooth Muscle Cell
SOC	Store Operated Channels
SOCE	Store-Operated Ca <sup>2+</sup> Entry
TG	Transglutaminase
TM	Thrombomodulin
TNF	Tumor Necrosis Factor
t-PA	Tissue-type Plasminogen Activator
TRPC	Transient Receptor Potential Channels
VE-cadherin	Vascular Endothelial Cadherin
vWF	von Willebrand Factor

## Abstract in German

Die chronisch thromboembolische pulmonale Hypertonie (CTEPH) ist eine seltene Erkrankung, bei der die Lungenarterien aufgrund der Ansammlung von thromboembolischem Material okkludieren und dadurch in den Pulmonalarterien ein erhöhter Lungendruck entsteht. Eine mögliche Behandlung dieser Erkrankung ist die chirurgische Entfernung des thromboembolischen Materials samt Neointima des Gefäßes. Dieser Eingriff wird als Pulmonale Endarterektomie (PEA) bezeichnet. Der zu entfernende Thrombus ist größtenteils fibrotisch und kollagenhaltig, weist jedoch nur eine geringe Rekanalisierung auf. Das Ziel dieser Studie war es, den Einfluss der Mikroumwelt und der Entzündungsmediatoren auf die Entwicklung und Stabilisierung des thromboembolischen PEA Materials zu untersuchen, welche zu chronischem Lungenhochdruck führen.

In dem PEA Material von CTEPH Patienten konnten wir muskularisierte und nicht-muskularisierte Gefäße entdecken. Die aus dem PEA Material isolierten Endothelzellen wiesen eine signifikante Veränderung ihrer Kalziumhomeostase im Vergleich zu gesunden humanen pulmonalen Endothelzellen (hPAECs) auf. Im Überstand vom PEA Material (FACS, ELISA) sowie auf Gewebesebene (histochemische Färbung) konnten wir die drei Faktoren Plateletfaktor 4 (PF4), Kollagen type I und Interferon-gamma-inducible 10kD protein (IP-10) detektieren. CXCR3, der Rezeptor für IP-10 und PF4, war vor allem im distalen Bereich des PEA Material erhöht exprimiert im Vergleich zu gesundem humanem Lungengewebe (RT-PCR). PF4, Kollagen typ I und IP-10 führten zu signifikanten Veränderungen in der Kalziumhomeostase sowie beeinflussten die Proliferation, Migration und Gefäßbildung in hPAECs.

In weiterem Verlauf konnten wir Entzündungsmediatoren, wie IL-8, MCP-1, IL-6, IP-10, RANTES, MIP1alpha and HMGB1 im Überstand und Gewebesebene vom PEA Material feststellen. Diese Faktoren waren, verglichen zu der gesunden Lunge und dem Serum von gesunden Donoren, ebenfalls hochreguliert auf mRNA bzw Serum Ebene. Ein Cocktail aus IL-8 , IL-6 und MCP-1 führte in hPAECs zu einer veränderten Kalziumhomeostase, wobei IL-8 eine Erhöhung in Proliferation und Migration hervorgerufen hat. Wir konnten auch zeigen, dass das Vorhandensein von angiostatischen Faktoren, wie z.B. PF4, Kollagen typ I und IP-

10 im PEA Material von CTEPH Patienten zu Veränderungen in der Kalziumhomeostase und zu endothelialen Dysfunktion führen kann. Trotz der ebenfallsigen Präsensts von angiogenischen Faktoren, wie IL-8 im PEA Material, scheint es, dass die angiostatischen Faktoren eine prominentere Auswirkung auf die Zellen im Thrombus haben. Basierend auf unseren Beobachtungen glauben wir, dass in den CTEPH Patienten die Balance von angiogenischen und angiostatischen Faktoren gestört ist, was zu einer Stabilisierung des Thrombus im Patienten führen kann.

## Abstract in English

Chronic thromboembolic pulmonary hypertension (CTEPH) is a rare disease with persistent thrombotic occlusion or stenosis of the large pulmonary arteries resulting in increased pulmonary pressure. Surgical removal of the neointimal layer of these vessels together with non-resolved thrombus consisting of organized collagen-rich fibrotic areas with partly recanalized regions is the treatment of choice (pulmonary endarterectomy, PEA). The aim of the study was to investigate the influence of the microenvironment and present inflammatory factors on the development and stabilization of the thromboembolic PEA material, leading to chronic pulmonary hypertension.

We observed muscularized and non-muscularized vessels in the PEA material. The isolated endothelial cells from the PEA material showed significantly different calcium homeostasis as compared to pulmonary artery endothelial cells (hPAECs) from normal controls. In the supernatant (FACS, ELISA) as well as in the tissue (histochemical staining) of the PEA material, platelet factor 4 (PF4), collagen type I and interferon-gamma-inducible 10 kD protein (IP-10) were detected. CXCR3, the receptor for IP-10 and PF4, was particularly elevated in the distal parts of the PEA material as compared to human control lung (RT-PCR). PF4, collagen type I and IP-10 caused significant changes in calcium homeostasis and affected proliferation, migration and vessel formation of hPAECs.

Additionally, we found IL-8, MCP-1, IL-6, IP-10, RANTES, MIP1alpha and HMGB1 in the supernatant of the PEA material and at tissue level. These factors were also up-regulated at mRNA and serum level compared to control lungs or serum from donors. The cocktail of the IL-8, MCP-1 and IL-6 lead to altered calcium homeostasis in hPAECs, whereas IL-8 specifically increased proliferation and migration of those cells.

The presence of angiostatic factors like PF4, collagen type I and IP-10 in the surgical PEA material from CTEPH patients may lead to changes in calcium homeostasis and endothelial dysfunction. Although also angiogenic factors such as IL-8 are present in the PEA material, the angiostatic factors might be more prominent. Based on our observations we suggest that the balance between angiogenic factors and angiostatic factors is disturbed in CTEPH patients, leading to the stabilization of the thrombi.

# Introduction

## Chronic thromboembolic pulmonary hypertension (CTEPH)

CTEPH is a rare and late possible consequence of venous thromboembolism. Up to 5,1% of people undergoing acute pulmonary thromboembolism develop CTEPH, whereas 40% of CTEPH cases lack a documented venous thromboembolic event (1). The diagnostic procedure and the management of patients with CTEPH have rapidly developed in the past decade. However the pathomechanism is still not completely understood.

The clinical picture of CTEPH shows, that due to the formation of the fibrotic occlusion in the pulmonary artery, patients suffer from increased pulmonary vascular resistance and show an elevated pulmonary artery pressure. The patients also show decreased oxygen absorption. The heart tries to overcome the decreased oxygen absorption by increased contractions, which leads to overstraining and enlargement of the right heart ventricle and often ends lethal due to right heart infarction (2,3).



**Fig.1:** Typical contrast enhanced 3D-MRA picture of the central enlarged pulmonary artery with multifocal stenoses of segmental arteries, reduction in diameter and vessel rupture. Arrows point to the occluded regions.

<https://www.thieme-connect.com/ejournals/pdf/roefo/doi/10.1055/s-2004-812998.pdf>

The acute pulmonary embolus can be resolved with the current antithrombotic therapy, which is sufficient to restore normal pulmonary hemodynamic, gas exchange and exercise tolerance under most circumstances. However, this does not indicate that complete restore of natural blood flow would occur (4). Miniati et al reported that only in 153 of 235 patients (65,1%) under treatment a normalization of the lung perfusion scan could be detected a year after a thromboembolic event (5). Auger and Fedullo postulated that the presence of

coexisting cardiopulmonary disease may contribute to the incomplete thromboembolic resolution leading to a so-called “pathological” state (4).

Growing evidence indicate that in the majority of the patients, the progressive rise in pulmonary vascular resistance (PVR) results not only from the occluded regions of the pulmonary artery, but also from pathophysiological changes in the distal pulmonary vascular bed. In lung biopsies, obtained at the time of pulmonary endarterectomy (PEA), it was found, that microvessels distal to both obstructed and non-obstructed central arteries develop histopathologic changes similar to those usually present in small-vessel pulmonary artery hypertension (PAH) (6). In addition, a poor correlation between the scintigraphic and angiographic extent of central thromboembolic obstruction and the severity of hemodynamic compromise was found (7,8). A recent study shows that in 10 to 15% of the patients who underwent a successful PEA, remodelling of the microvessels distal from the clot occurs, leading to a persistent PAH. In some patients, the PAH has even progressed in the absence of perfusion scan changes or evidence of embolic recurrence (4).

The CTEPH patients who are excluded from the PEA due to high risk factors such as non-reachable distal localization of the clots, have to be treated via medication. The same is true for patients with persistent postoperative PAH. Some studies have shown that both groups show a benefit from vasodilating/antiproliferative medications such as prostacyclin analogs, endothelin receptor antagonists, and phosphodiesterase-5 inhibitors (9-11). Although indication for the use of these therapies in CTEPH and associated efficacy has not yet been clearly established, an increase in prescription even in operable CTEPH patients could be observed over the last years (4).

### **Misguided thrombus resolution**

The first pathogenic component of CTEPH is the primary obstruction of the central pulmonary arteries by accumulation of thrombotic material and the second is severe pulmonary vascular remodelling. It has been postulated that the reason for the development of the persistent occlusion in the pulmonary artery is a misguided thrombus resolution triggered by infection, inflammation, autoimmunity, malignancy (12) and/or endothelial dysfunction (13). The clot consists of different

cell types, such as pulmonary artery smooth muscle cells (PASMC), endothelial cells (PAEC) and myofibroblasts expressing vimentin and alpha smooth muscle actin. The predominant phenotype in the thrombotic material is the myofibroblast cell type, which might transdifferentiate from adventitial fibroblasts or mesenchymal progenitor cells. In addition, multipotent mesenchymal progenitor cells were detected in the PEA tissue (14). The detected remodelling and vessel wall thickening of pulmonary arteries in CTEPH patients, who underwent lung transplantation, might be partly explained with excessive PASMC proliferation, where store-operated  $Ca^{2+}$  entry (SOCE) and transient receptor potential channels (TRPC) are known to play a role (15,16).

The fibrotic thrombus consists of an organized fibrin structure (17). In proximal regions of the clot  $\alpha$ -actin positive stained PASMC are localized. Neoangiogenesis and recanalization occurs in distal regions of the thromboemboli. Endothelial progenitor cells are present in the proximal and distal areas, whereas inflammatory cells (ex.  $CD45^+$ ) and collagen-secreting cells are in the proximal vascular wall. It is suggested, that the differentiation of adventitial fibroblasts or mesenchymal progenitor cells present in the neointima of the occluded vessels of CTEPH patients might be triggered by factors present in the microenvironment of the clot (14).

The reason for the misguided resolution of the clot or resistance to conventional, anticoagulant and vasodilator treatment is currently unknown. However, the resistance to thrombolysis could be explained by the polymorphism affecting the fibrinogen  $\alpha$ - $\alpha$  chain cross linkage. It has been found that particularly the beta-chain N-terminus of fibrin from CTEPH patients was resistant to thrombolysis (18-21). Interestingly, CTEPH patients who underwent PEA show significantly increased thrombomodulin (TM) concentrations in the plasma. TM is an endothelial surface protein. TM binds thrombin and acts as a cofactor for the conversion of protein C to its activated form, which is a natural anticoagulant. The significantly increased amount of TM after PEA could point to an endothelial dysfunction in addition to a prothrombotic state in the pre-PEA patients (22).

The stabilized clot not only occludes the vessel, but also acts as a “physical” trap for circulating mitogenic, inflammatory and vasoactive factors. These factors can also lead to endothelial dysfunction as described by Sacks et al. They have shown that the occluded vessels undergo changes in shear stress leading to altered

endothelial functions by producing and releasing vasoactive factors (23). Furthermore, the microenvironment, for example thrombin, potently affects endothelial cells leading to mobilization of  $\text{Ca}^{2+}$ , rearrangements of the cytoskeleton and resulting in endothelial dysfunction (24).

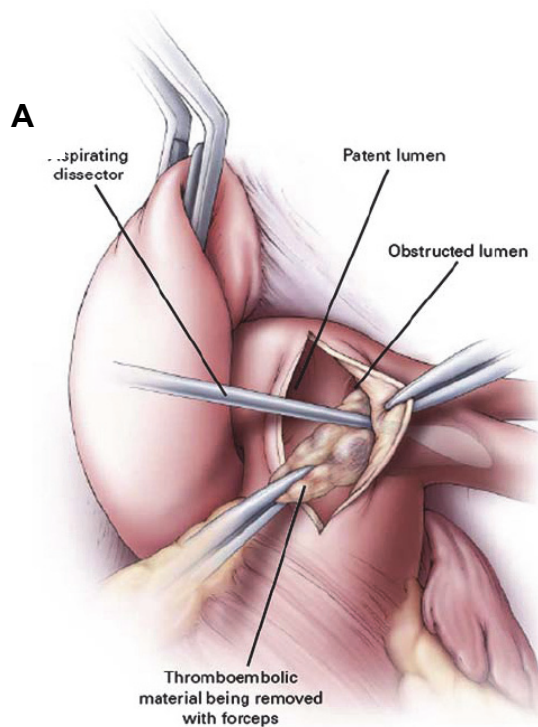
An elegant study about arterial chronic total occlusion (CTO) in rabbits shows three different stages: early (2 weeks), intermediate (6 to 12 weeks) and advanced (18 to 24 weeks) of chronic thrombus development (25). In the first stage acute inflammation as well as myofibroblast infiltration within the thrombotic occlusion plays a role, which is characterized by abundant proteoglycans and low collagen density. In the initial intermediate stage neovascularisation accompanied by increased CTO perfusion occurs, whereas at later intermediate stage the number of microvessels and relative blood volume within the CTO already decreases. This process continues into the advanced stage. The consistence of the clot changes over time from initially proteoglycan-rich extracellular matrix into a collagen-rich scar stage (8,25). These observations could be a hint indicating that the microenvironment, formed after several weeks, may act angiostatic on the endothelial cells and therefore may alter the recanalization-process of the clot.

### **Pulmonary endarterectomy (PEA)**

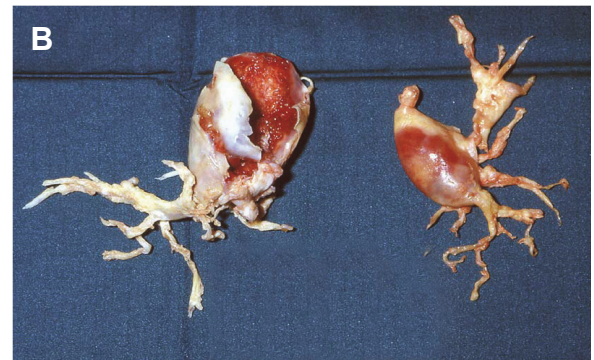
PEA almost normalizes the cardiopulmonary function of CTEPH patients. During the surgical procedure the organized and incorporated fibrous obstructive tissue is removed from the pulmonary arteries. During surgery median sternotomy, cardiopulmonary bypass, deep hypothermia and circulatory arrest are applied. For the surgical outcome it is crucial to remove all thrombotic material. The accessibility of the thrombi and therefore the success of thrombus removal depend to a large degree on the surgical team's expertise (26).

The clinical guidelines for the selection of the patients for the PEA are given by the American College of Chest Physicians. The CTEPH patients should show New York Heart Association (NYHA) functional class III or IV symptoms (27) and should have a preoperative pulmonary vascular resistance (PVR) greater than  $300 \text{ dyn}\cdot\text{s}\cdot\text{cm}^{-5}$  (28). An important point is the accessibility of the thrombus in the main lobar or segmental pulmonary arteries as well as the absence of severe co-morbidities (29,30);. For example, severe underlying chronic lung disease, either

obstructive or restrictive would speak against the surgery. A mean pulmonary artery pressure of 40 mmHg or greater, level of surgical experience and the presence or absence of advanced secondary arteriopathy influence the decision for PEA selection (31). A reduction of pulmonary resistance of more than 50% should be possible in the patients who are scheduled for PEA (32).



(Fedullo, Auger et al. 2001)



(Mayer, Klepetko 2006)

**Fig.2:**  
(A) PEA surgical method (B) PEA tissue.

To be able to perform the PEA, the patient has to be put under total circulatory arrest and cooled down to 18-20°C. This is important to maintain a clear view in the distal pulmonary arterial branches, otherwise back-bleeding would occur due to development of a systemic-to-pulmonary artery circulation at the precapillary level (13). The total time of circulatory arrest is normally less than 40 min however, it should not exceed 50 to 60 min. For the clinical outcome of the PEA it is crucial to find the right dissection plane, neither to perforate the artery nor to dissect in a too superficial plane. After removal of the endarterectomised tissue, the patient is reperfused and slowly warmed up back to 37°C (26).

The patients who underwent PEA can be classified, according to their surgical specimens, into four groups. Type 1 had fresh thrombus in the main lobar pulmonary arteries, type 2 showed intimal thickening and fibrosis proximal to the

segmental arteries, type 3 had disease within distal segmental arteries only and type 4 showed distal arteriolar vasculopathy without visible thromboembolic disease (33).

The mortality rate of patients who underwent PEA ranges between 4 to 24% (29,34) depending on the centre. In a retrospective study of Darteville et al., the main reason for death was the persistent pulmonary hypertension (17 out of 275; 60,7% of all operative deaths n=28), followed by pulmonary edema (3 patients) and pneumopathy (3 patients) (13). In addition, a correlation between the hemodynamic severity and operative mortality rate from PEA was observed. High preoperative PVR of the patients corresponds to high mortality rate. Darteville et al also reported a mortality rate of 4% in patients with a preoperative PVR of less than  $900 \text{ dyn}\cdot\text{s}\cdot\text{cm}^{-5}$ , whereas between 900 and  $1200 \text{ dyn}\cdot\text{s}\cdot\text{cm}^{-5}$  the mortality rate raised up to 10%. In patients with even higher PVR values the mortality rate went up to 20% (13). There are additional factors, which can influence the surgical outcome. For example a high operative risk is given, when the patients show no history of acute thromboembolic event, hemodynamic angiographic imbalance is present, the thrombotic material is located distal, an indwelling catheter is present and/or the patients suffer of myeloproliferative syndrome. In contrast, factors speaking for a surgical success are following: the patient has a prior history of pulmonary embolism and/or deep vein thrombosis, or a so-called honeymoon period, which means that months or years lay between the embolic event and clinical symptoms (26).

It can be concluded, that PEA is a complex surgical procedure, which can be considered curative by providing significant and sustained functional and hemodynamic improvement in the majority of CTEPH patients. Due to the dependence of the postoperative outcome on surgical expertise the mortality rates continue to decrease.

### **Vascular endothelial cells**

The inner monolayer of the lung artery, frequently referred as the pulmonary artery, is formed by the pulmonary artery endothelial cells (PAECs), constructing a semipermeable barrier between the blood and the tissue (35-37). Signals sent

from hPAECs to the surrounding smooth muscle cells (SMCs) can lead to vessel constriction or vasodilatation.

The endothelial cells play a major role in anti-thrombotic reactions and intravascular coagulation inhibition in the systemic as well as in the pulmonary circulation. The endothelium releases besides prostacyclin (PGI<sub>2</sub>) (38) and nitric oxide (NO) (39), the tissue-type plasminogen activator (t-PA) (40), which induces fibrinolysis. The direct transformation of plasminogen into plasmin performed by this serine-protease normally inhibits the blood coagulation. In a pro-thrombotic endothelium and in CTEPH patients less t-PA is released (41). Instead of t-PA release, the plasminogen-activator inhibitor (PAI-1) is secreted in an increased amount (42). The fibrinolysis is therefore perhaps inhibited and thrombus may occur more frequently (34).

Calcium is an important physiological regulator in the endothelial cells. It is a widely ranging signal, influencing cellular motility, cell growth, proliferation, enzyme activity, and permeability of ion channels, activity of ion pumps and components of the cytoskeleton. An increase in the cytoplasmic calcium level can be evoked by several signals from the blood flow, which can be of physical or chemical origin (43). These stimuli often lead to an increase of the intracellular cytosolic calcium level (44-49).

A rise in the intracellular calcium level; e.g. induced by inflammatory mediators; regulates and initiates a wide range of cellular events in endothelial cells as well as in the surrounding smooth muscle cells (36). In the endothelial cells this intracellular calcium rise can occur by depletion of the sarco-endoplasmic reticulum (SER) or via influx from the extracellular space through store or receptor operated channels (SOC or ROC) (36).

The depletion of calcium from the SR-stores leads to an increase of intracellular calcium, which activates plasma membrane located calcium channels (36,50,51). From the extracellular space calcium enters through these store-operated channels (SOCs) (36). Besides SOCs other TRPC-encoded receptor operated channels (ROCs) exist in the plasma membrane of endothelial cells. To maintain the calcium homeostasis of the cell, the calcium stores are refilled by the sarco/endoplasmic reticulum calcium ATPase (SERCA). This is a calcium pump,

which is located in the SR-membrane and is responsible for cytosolic  $\text{Ca}^{2+}$  balance (52).

Adherent junctions play an important role in directing the morphogenesis of the vasculature during angiogenesis. These structures could be important not only for the cell assembly, but also for the overall architecture of the vasculature (53). For sprouting and lengthening of the vessel, the expression of cell surface proteins by the endothelial cells is needed. For example vascular endothelial cadherin (VE-cadherin), which is only expressed by endothelial cells, promotes cell adhesion by a calcium dependent homotypic mechanism. In the presence of calcium the VE-cadherin from one cell binds to the VE-cadherin from the neighbouring one (54).

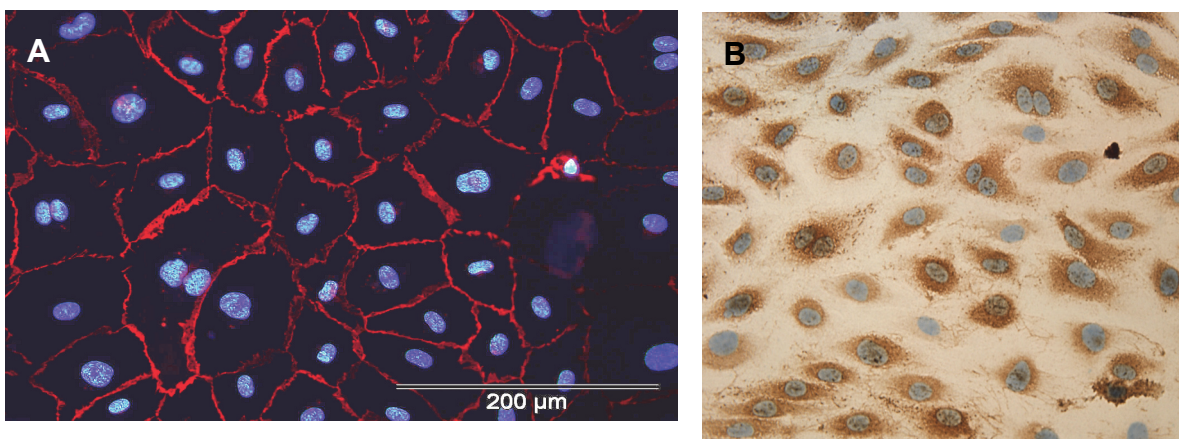


**Fig.3:** (A) VE-cadherin and (B) vWF staining on CTEPH-hECs

A typical marker for endothelial cells is the von Willebrand Factor (vWF), which is a blood glycoprotein (gp) and plays an important role in haemostasis. It is constantly produced by the endothelium in the Weibel-Palade bodies, megakaryocytes and subendothelial connective tissue. vWF has different roles *in vivo*, one of the most important is the binding of factor VIII, which is inactive when bound and its degradation gets retarded. Factor VIII gets free from vWF upon the action of thrombin and therefore activated. vWF binds beside Factor VIII also collagen when, due to blood vessel damage, it gets exposed to the endothelial cells. Under high shear stress (i.e. blood flow in narrow blood vessels) the most

efficient binding of vWF to platelet gpIb occurs when it builds a complex with gpIX and gpV. It also binds to other platelet receptors when they are activated by thrombin for example during coagulation process. Due to the fact that vWF plays a crucial role in blood coagulation, a deficiency or dysfunction can lead to bleeding tendencies e.i. in tissue with high shear stress, vWF than uncoils and slows down passing platelets (55).

## **Aim of the study**

- 1.** To characterise the histology of the fresh PEA material of CTEPH patients.
- 2.** To investigate the reason for the misguided resolution of the thrombotic clot in CTEPH patients. For this purpose endothelial cells isolated from the PEA tissue will be compared to healthy hPAEC to explore possible factors of endothelial dysfunction.
- 3.** To analyze the role of the microenvironment on the endothelial function. In order to show this we will investigate the effect of IP-10, collagen and platelet factor 4, which are present in PEA tissue, on vessel formation, migration, proliferation and permeability in hPAECs.
- 4.** To study the presence of inflammatory factors in the PEA surgical material and their effect on hPAECs  $\text{Ca}^{2+}$  handling.
- 5.** To investigate inflammatory factors in the serum of CTEPH patients compared to healthy donors and their possible influence on fibroblast migration.

## **Material and Methods**

### **Isolation of primary human endothelial cells from PEA material**

Endothelial cells were isolated from the endarterectomised tissue of chronic thromboembolic pulmonary hypertension (CTEPH) patients (n=38) undergoing pulmonary endarterectomy (PEA). The study protocol for tissue donation was approved by the Institutional Review Board of the Medical University of Vienna (Ek-Nr: 903/2009) in accordance with national law and with guidelines on Good Clinical Practice/International Conference on Harmonization. Written informed consent was obtained from each individual patient.

The PEA material was carefully cut into small pieces under microscopic guidance and placed into 75 cm<sup>3</sup> culture flasks with a drop of endothelial cell (EC) culture media (VascuLife® VEGF Cell Culture Medium; LifeLine Technology, Walkersville). The tissue with the outgrowing cells was maintained at 37°C and 5% CO<sub>2</sub>. After 24h the media was filled up to 15ml and then changed every 48h thereafter. For purifying the EC culture, magnetic bead sorting with CD31 antibodies (91935, Milteny) on MACS® was performed using the POSSEL program. The received, pure CTEPH-hEC identity was verified by characteristic appearance in phase-contrast microscopy, followed by immunocytochemical stainings for von Willebrand factor (vWF) (dilution 1:100, Dako) and vascular–endothelial cadherin (VE-cadherin) (1:200, Santa Cruz).

### **Isolation of adventitial fibroblasts from donor lungs**

Adventitial fibroblasts were isolated from pulmonary arteries from non-transplantable donor lungs, by removing the adventitial layer. The adventitial fibroblast tissue was cut with the three scissor technique into very small fragments. The fragments were resuspended in adventitial Fibroblast medium (FibroLife Medium with FibroLife S2, LS-1038 supplements; LifeLine) and cultured in T75 culture flasks.

## **Immunohistochemistry**

Fresh surgical material from pulmonary endarterectomy (PEA) was fixed in 4% formaldehyde for 24h and embedded in paraffin blocks. The sliced paraffin tissue (2µm thick) was placed on Capillary Gap Microscope Slides (Dako REAL™) and kept for further use at room temperature. For single or double staining, as primary antibodies von Willebrand factor (dilution 1:100; Dako) and/or  $\alpha$ -Actin (dilution 1:100; Sigma) and as secondary antibodies goat-anti-rabbit-HRP (dilution 1:100; Santa Cruz Biotechnologies) or goat-anti-mouse-HRP (dilution 1:100; Santa Cruz Biotechnologies) were used. For CD31 staining (dilution 1:100; Abcam) the DAB detection kit from R&D Systems was applied. The immunohistochemical stainings for CXCR3 (1:250, ab64714), CXCR2 (1:100, ab14935) IP-10 (1:250, ab9807), PF4 (1:250, ab49735), IL-8 (1:100; ab7747), MCP-1 (1:100, ab73680) or IL-6 (1:100, ab6672) were performed with the same kit. For the Haematoxylin Eosin (H.E.) staining the protocol after Gill was used. The staining was analyzed in single blinded manner by a pathologist. For the collagen fibre staining the Masson's Trichrome staining protocol was used according to the manufacturer's instructions. The stainings for vimentin (1:100, ab11256),  $\alpha$ -Actin (1:500, Everest Biotech) and fibronectin (1:250, ab23750) were performed with the Vektor ImmPRESS reagent kit.

## **Flow-cytometric analysis**

After removal, the PEA samples from CTEPH patients (n = 8) were immediately put in endothelial cell basal medium supplemented with 5% FCS and antibiotics (VascuLife® VEGF Cell Culture Medium; LifeLine Technology, Walkersville). The tissue was cut into small pieces and incubated for 18h at 37°C in DMEM-F12 medium with 0,3% FCS, 1% Glutamin, 1% penicillin and streptomycin. The supernatant was collected and stored at -80°C; afterwards the tissue was briefly washed with Hepes buffer and lysed in 150µl RIPA buffer with PhosphoStop and Protease Inhibitor Complex. The supernatant of the PEA tissue, the serum of CTEPH patients and donors were checked for the presence of inflammatory factors such as IL-8, RANTES, MIG, MCP-1, IP-10, IL-2, IL-4, IL-6, IL-10, TNF, IFN-g (Human Chemokine Kit Cytometric Bead Array (CBA); Human Th1/Th2

Cytokine Kit II Cytometric Bead Array; BD Bioscience) with a flow-cytometer (FACS Canto II, Becton Dickinson, Franklin Lakes, NJ). For measuring MIP1 $\alpha$  in the PEA supernatant and serum from CTEPH patients and donors, human MIP1 $\alpha$  Flex set (Cytometric Bead Array; BD Bioscience) was applied.

## **ELISA**

For the quantitative measurement of PF4 and Collagen type I in the supernatant of PEA tissue an in vitro enzyme-linked immunosorbant assay (ELISA kit from RayBio; Cat#: ELH-PF4-001) or a competitive EIA (ELISA kit from Cosmo Bio Co.; ACE-EC1-E205 EX) was used. Each well of a 96-well microtiter plate already pre-coated with anti-human PF4 was incubated with 100 $\mu$ l of test solution overnight (4°C). After triple washing steps the biotinylated antibody was added for 1h RT with gentle shaking. After repeated washing steps 100 $\mu$ l Streptavidin solution was added on each well for 45min at RT. 100 $\mu$ l TMB One-Step Substrate Reagent was applied for 30min RT in dark. The reaction was then stopped and plates were read at 450nm immediately (For details see RayBio Human PF-4 ELISA Kit protocol). In case of human collagen type I ELISA assay the samples were labelled with biotinylated anti-collagen antibody solution after washing for 1h at RT. Avidin HRP conjugate were added and detection was performed similar to the quantitative ELISA with TMB substrate according to the manufacturer instructions. The absorbance of the colour density of the reaction mixture was measured at 450nm with a photometer (Molecular Devices, SPECTRAMax Plus 384). For the quantification of CXCL12 and HMGB1 in the supernatant of PEA tissue and in the serum of CTEPH patients an immunoassay was performed according the assay instructions (Human CXCL12/SDF-1 $\alpha$ , R&D systems; HMGB1 ELISA, IBL).

## **RNA-isolation and PCR**

Total cellular RNA from hPAECs (CC-2530, Lonza) was isolated with the RNeasy Mini Kit from Qiagen. For RNA isolation from PEA tissue and human lungs the Trizol protocol was applied. A Nanodrop 2000c spectrophotometer (PeQlab) was used to quantify the concentration and the purity of the isolated total RNA. The total RNA was converted to cDNA using a RevertAid H Minus First Strand cDNA

Synthesis kit (Fermentas). PCR amplifications were performed by Lightcycler 480 (Roche). Cells were used between passage 4 and 8 for experiments.

## **Proliferation**

CTEPH-hECs and hPAECs (CC-2530, Lonza) were seeded on 6 well plates with a starting cell number of 20.000. The cells were grown for 4 and 8 days; afterwards they were collected by trypsinisation and counted by CASY (Schärfe system).

To additionally investigate the effect of different stimuli on hPAECs the following protocol was applied: 5.000 hPAECs were seeded in 96 well plates, the following day the cells were treated for 24h with 100ng/ml or 400ng/ml IL-8, 600ng/ml IP-10, 1000ng/ml PF4, 100µg/ml Collagen type I or kept in control conditions (VascuLife® Basal Medium with 2%FCS; LifeLine Technology, Walkersville). The growth and proliferation of hPAECs was determined by [<sup>3</sup>H]thymidine (ART-0178A-1, BIOTREND Chemikalien GmbH) incorporation as an index of DNA synthesis and the radioactivity was measured by a scintillation counter (Wallac 1450 MicroBeta TriLux Liquid Scintillation Counter & Luminometer). Cells were used between passage 4 and 8 for experiments.

## **Vessel formation assay**

To test the angiogenic property of the endothelial cells (ECs) an In Vitro Angiogenesis Assay Kit (ECM625, Millipore) was used. A matrigel was prepared in a 96 well plate according to the manufacturer's instructions. In each well 16.000 cells were seeded out on this gel. After 21h, pictures were taken with a light microscope (Zeiss epifluorescent 4X). The numbers of formed branching points were counted.

To test the effect of IL-8 (100ng/ml), PF4 (400ng/ml), IP-10 (600ng/ml) and Collagen type I (100µg/ml) on hPAECs phase contrast pictures were taken with the light microscope after 6h of stimulation (Zeiss epifluorescent 4X). The number of formed loops were counted and compared to control cells (cultured only in full media). Cells were used between passage 4 and 8 for experiments.

## **Wound healing assay**

CTEPH-hECs and hPAECs were cultured until confluence in 12 well plates. At the start of the experiment (0h), a longitudinal wound was applied with a 1ml blue pipette tip. The scratch resulted in a cell-free gap of approximately 1.0mm between the adjacent areas of the cells. The migrating cells were monitored in a Zeiss Cell Observer and pictures were taken every 2h for 72h with a 10X objective. The results were analyzed via measuring the cell-free area at a given time point and were normalized to the 0h size.

For investigating the effect of different stimuli on hPAEC, the cells were cultured until confluence in ibidi culture inserts for 24-well plates. By removing the inserts a wound of approximately  $400\mu\text{m} \pm 50\mu\text{m}$  was applied. The cells were then stimulated either with 100ng/ml IL-8, 600ng/ml IP-10, 400ng/ml PF4 or 100 $\mu\text{g}/\text{ml}$  Collagen type 1 for 36h or kept in control conditions (EC-culture media) ( $t_0$ ). The results were analyzed via measuring the actual wound size at a given time point ( $t_{36\text{h}}$ ), normalized to the 0h size and expressed as % of closed wound. Cells were used between passage 4 and 8 for experiments.

## **Permeability measurement with fluorescently labelled dextran**

To assess the permeability changes of the endothelial monolayer, hPAECs were grown until confluence on semi-permeable inserts (Millipore) and incubated for 1h or 6h with 400ng/ml PF4, 600ng/ml IP-10, 100 $\mu\text{g}/\text{ml}$  Collagen type I or control solution. After treatment, FITC-labelled dextran (FD2000S, Sigma) was added to the upper compartment of the insert and after 10min the fluorescence of the solution from the bottom well was measured with a fluorimeter (BMG LabTech, FLUOstar OPTIMA). Cells were used between passage 4 and 8 for experiments.

## **Live cell $\text{Ca}^{2+}$ imaging**

CTEPH-hECs and hPAECs (CC-2530, Lonza) were cultured on 25mm diameter, gelatine-coated glass cover slides until confluence. After incubation, the cells were loaded in dark for 45 minutes with 2 $\mu\text{M}$  fura-2/AM and washed with Ringer solution (5,8mM KCl, 141mM NaCl, 0,5mM  $\text{KH}_2\text{PO}_4$ , 0,4mM  $\text{NaH}_2\text{PO}_4$ , 11,1mM glucose,

10mM Hepes, 1,8mM CaCl<sub>2</sub>, 1mM MgCl<sub>2</sub>, pH 7,4). After 15 minutes the single glass cover slide was mounted on the stage of a Zeiss 200M inverted epifluorescence microscope coupled to a PolyChrome V monochromator (Till Photonics) light source in a sealed, temperature-controlled RC-21B chamber (Warner Instruments). Fluorescence images were obtained with alternate excitation at 340 and 380nm. Emitted light was collected at 510nm by an Andor Ixon camera. The acquired images were stored and subsequently processed offline with TillVision software (Till Photonics). During the measurement the cells were perfused with 10µM histamine or 15µM 1,4-dihydroxy-2,5-di-tert-butylbenzene (BHQ: selective SERCA blocker) in the presence or absence of extracellular calcium.

Measurements were made every 3s. Background fluorescence was recorded from each cover slip and subtracted before calculation. Maximal and minimal ratio values of the [Ca<sup>2+</sup>]<sub>i</sub> were determined at the end of each experiment by first treating the cells with 1 µM ionomycin (maximal ratio) and then chelating all free Ca<sup>2+</sup> with 20 mM EGTA (minimal ratio). Cells that did not respond to ionomycin were discarded. [Ca<sup>2+</sup>]<sub>i</sub> was calculated as described by Grynkiewicz et al (56). To determine the intracellular calcium concentration the following equation was used:

$$[Ca]_i(nM) = K_d \times \beta \times \frac{Ratio_{340/380} - R_{min}}{R_{max} - Ratio_{340/380}}$$

$K_d$  = 224 nM, is the dissociation constant of Fura-2;

$\beta = \frac{F_{380 \text{ max}}}{F_{380 \text{ min}}}$  signal from the 380nm excitation;

$R_{min}$  is the minimal ratio, determined by 20mM EGTA;

$R_{max}$  is the maximal ratio, determined by 1µM ionomycin;

$Ratio_{340/380}$  is the ratio of the fluorescence at 340nm and 380nm excitation.

For the live cell Ca<sup>2+</sup> imaging data analysis, the basal level of Ca<sup>2+</sup> was determined as an average value of the first 50 seconds of the curve. Afterwards, the agent-induced Ca<sup>2+</sup> peak height after subtracting the baseline as well as the duration of the Ca<sup>2+</sup> response were quantified. The latter is the time from the maximum Ca<sup>2+</sup> peak height until the intracellular Ca<sup>2+</sup> declines to the basal level.

## Chemotaxis assay / Transwell migration

Oregon green stained hPAECs were seeded on top of 8µm pore size filters (Millipore) for 5h. In the bottom of the well 2% EC basal medium alone or with 100ng/ml or 400ng/ml IL-8, 400ng/ml PF4, 600ng/ml IP-10 and 100µg/ml collagen was added. 10X pictures of 5 different regions for each filter were made with a fluorescent microscope. The number of cells, which migrated after 5h on the bottom side of the filters were counted.

## Statistical analysis

Numerical values are given as means ± SEM of n cells unless otherwise stated. Intergroup differences were assessed by factorial analysis of variance with post hoc Bonferroni test. P-values < 0.05 were considered significant.

## Primers, Antibodies and Substances

### Primers:

Gene name	Forward primer (5' - 3')	Reverse primer (5' - 3')
huIL10	ATGCTCCTAGAGCTGCGGACT	CCTGCATTAAGGAGTCCGGTTAG
huIL2	ACA GCT ACA ACT GGA GCA TT	TGC TGT CTC ATC AGC ATA TT
huIL4	CTG CAA ATC GAC ACC TAT TA	GAT CGT CTT TAG CCT TTC
huMIG	TTA AAC AAT TTG CCC CAA GC	CTG TTG TGA GTG GGA TGT GG
huIFNgamma	GCATCCAAAAGAGTGTGGAG	GCAGGCAGGACAACCATTAC
huIL-8	ATAAAGACATACTCCAAACCTTTCCAC	AAGCTTTACAATAATTTCTGTGTTGGC
huIP-10	TGACTCTAAGTGGCATTCAAGGAG	TTTTTCTAAAGACCTTGATTAACAGG
huIL-6	GTAGCCGCCCCACACAGA	CATGTCTCCTTTCTCAGGGCTG
huTNF-alpha	CCCAGGGACCTCTCTAATCA	GCTTGAGGGTTTGCTACAACATG
huRANTES	TTTGCCTACATTGCCCGC	TTTCGGGTGACAAAGACGACT
huMCP-1	ACTCTCGCCTCCAGCATGAA	TTGATTGCATCTGGCTGAGC
huCXCL12	5-TGCCAGAGCCAACGTCAAG	5-CAGCCGGGCTACAATCTGAA
huCx3cl1	5-CCTGTAGCTTTGCTCATCCACTATC	5-CCAAGATGATTGCGCCTTT
huCx3cr1	5-TGACTGGCAGATCCAGAGGTT	5-GTAGAATATGGACAGGAACAC
huCXCR4	5-TGACGGACAAGTACAGGCTGC	5-CCAGAAGGGAAGCGTGATGA
huCCR3	5-ATGACAACCTCACTAGATACAGTTG	5-CTAAAACACAATAGAGAGTTCCGGC
huCCR4	5-CACACATACTGCAAACCCAGTA	5-TCCAGGGAGCTGAGGACTT
huCCR5	5-CAAAAAGAAGGTCTTCATTACACC	5'-CCTGTGCCTCTTCTTCTCATTTCG
huHMGB1	5'-TATGGCAAAGCGGACAAGG	5'-CTTCGCAACATCACCAATGGA

Gene name	Company	Product Nr.
huCXCR1	Qiagen	Hs_CXCR1_1_SG QuantiTect Primer Assay (200)
huCXCR2	Qiagen	Hs_CXCR2_1_SG QuantiTect Primer Assay (200)
huCXCR3	Qiagen	Hs_CXCR3_1_SG QuantiTect Primer Assay (200)
huCXCR5	Qiagen	Hs_CXCR5_1_SG QuantiTect Primer Assay (200)
huCCR2	Qiagen	Hs_CCR2_2_SG QuantiTect Primer Assay (200)
huIL6R	Qiagen	Hs_IL6R_1_SG QuantiTect Primer Assay (200)
huCOL4A3	Qiagen	Hs_COL4A3_1_SG QuantiTect Primer Assay (200)
huCXCL10	Qiagen	Hs_CXCL10_1_SG QuantiTect Primer Assay (200)
huPF4	Qiagen	Hs_PF4_1_SG QuantiTect Primer Assay (200)
huB2M	Qiagen	Hs_B2M_1_SG QuantiTect Primer Assay (200)

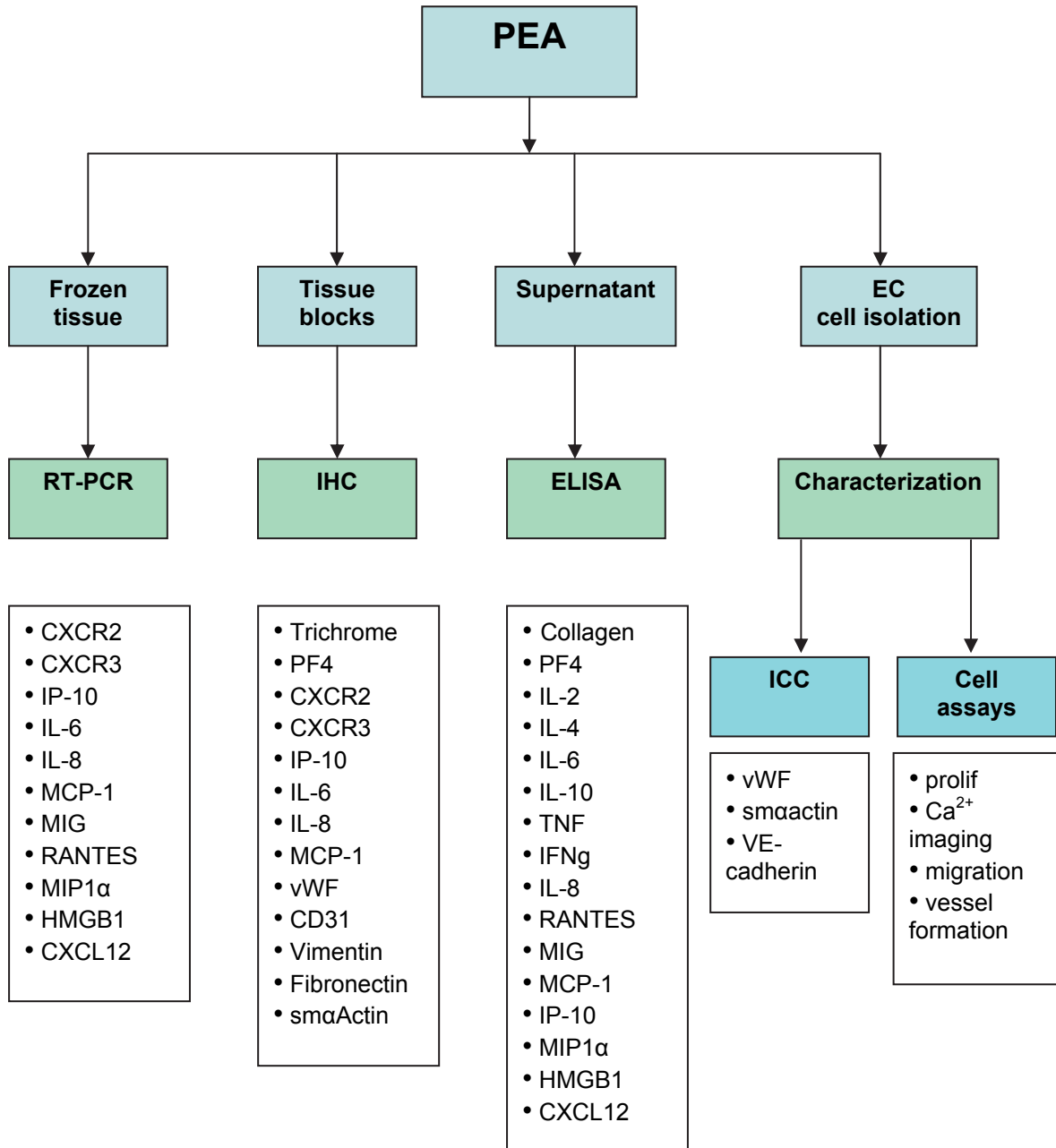
### Antibodies:

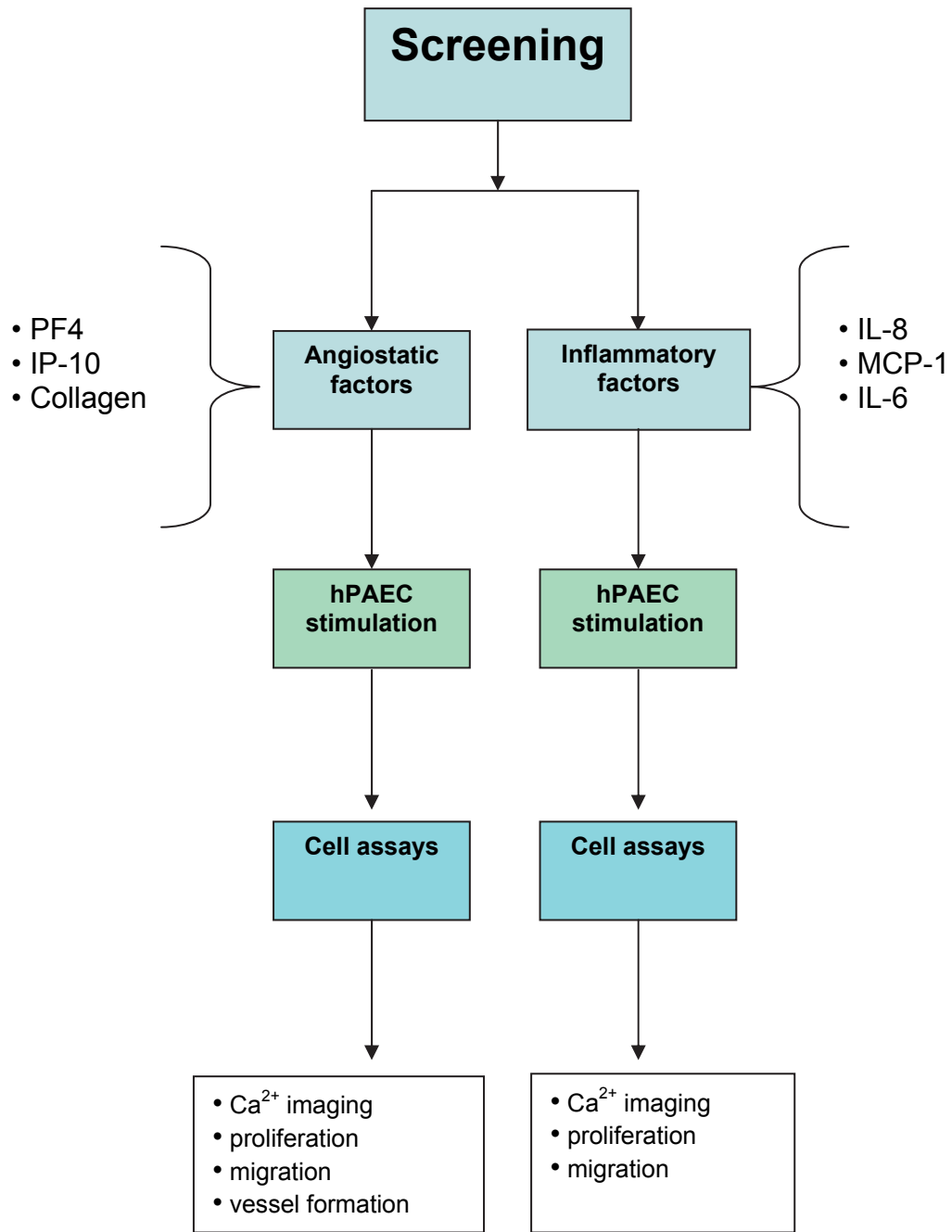
Antibody	Isotype	Dilution	Company	Product Nr.
CD31 Micro Beat Kit Human	rb	1to50	Milteny	91935
CD31 Antibody	rb	1to100; PH9	abcam	ab32457
vWF	rb	1to100	Dako	
vWF	ms	1to200	Dako	
VE cadherin	ms	1to200	Santa Cruz	
CXCR2	rb	1to100; PH6	abcam	ab14935
CXCR3	ms	1to250; PH6	abcam	ab64714
CCR2	rb	1to100; PH6	abcam	ab32144
IL6	rb	1to100; PH6	abcam	ab6672
IL8	rb	1to100; PH9	abcam	ab7747
MCP-I	rb	1to100; PH6	abcam	ab73680
IP-10 ; CXCL10	rb	1to250; PH6	abcam	ab9807
PF4	ms	1to250; PH9	abcam	ab49735
Vimentin	goat	1to100; PH9	abcam	ab11256
Fibronectin	rabbit	1to250; PH9	abcam	ab23750
$\alpha$ actin	goat	1to500	Everest Biot	EB06450

### Substances:

Substances	Company	Product Nr.
Collagen Solution Type1	Sigma	C3867
BHQ	Sigma	
Histamin	Sigma	
EGTA	Sigma	
Ionomycin calcium salt	Sigma Aldrich	I3909
Recombinant Human IL8 (72aa) (CXCL8)	Peptotech	200-08M
Recombinant Human IL6	Peptotech	200-06
Recombinant Human MCP-1 (CCL2)	Peptotech	AF-300-04
Recombinant Human PF-4 (CXCL4)	Peptotech	300-16
Recombinant Human IP-10 (CXCL10)	Peptotech	300-12
Recombinant Human MIG (CXCL9)	Peptotech	300-26
FITC-dextran	sigma aldrich	FD2000S
autoMACS columns	Miltenyi Biotec	130-021-101
autoMACS Rinsing solution	Miltenyi Biotec	130-091-222
autoMACS Running Buffer	Miltenyi Biotec	130-091-221
Vascular Endothelial Growth Factor human	sigma aldrich	V7259-10UG
Oregon green 488 carboxylic acid diacetate	Invitrogen	O34550

# Flow chart of work sequence





# Results

## **PART1**

---

### **Characteristic parameters of CTEPH patient population**

The characteristics of the patient population from where the PEA surgical tissue was obtained are shown in Table 1.

*Table 1: Patient characteristics (Data are shown as mean±SD or mean (range))*

	<b>CTEPH (n= 38)</b>
<b>Age (years)</b>	55 (21-78)
<b>Gender (female, %)</b>	40
<b>mPAP preoperative (mmHg)</b>	53 ± 13.6
<b>PVR preoperative (dyn·sec·cm<sup>-5</sup>)</b>	923 ± 396
<b>CO preoperative (L·min<sup>-1</sup>)</b>	4.4 ± 0.8
<b>CI preoperative (L·min<sup>-1</sup>·m<sup>-2</sup>)</b>	2.2 ± 0.3

### **Characteristic appearance of PEA surgical material of CTEPH patients**

The PEA surgical material has an organized, but highly diverse structure. Examining the HE staining taken from different tissue areas of a single patient (Fig.4), the difference in the composition as well as the cell allocation is obvious. For example, distal areas of the clot are highly organized, which is visible by the presence of connective tissue, collagen richness and high cell number (Fig.4 A, B), the latter shown by the amount of blue nuclear staining. Coming to the proximal areas, where the thrombotic material freshly accumulates from the circulation, high fibrin presence is typical, as well as reduced cell number (Fig.4 C, D).

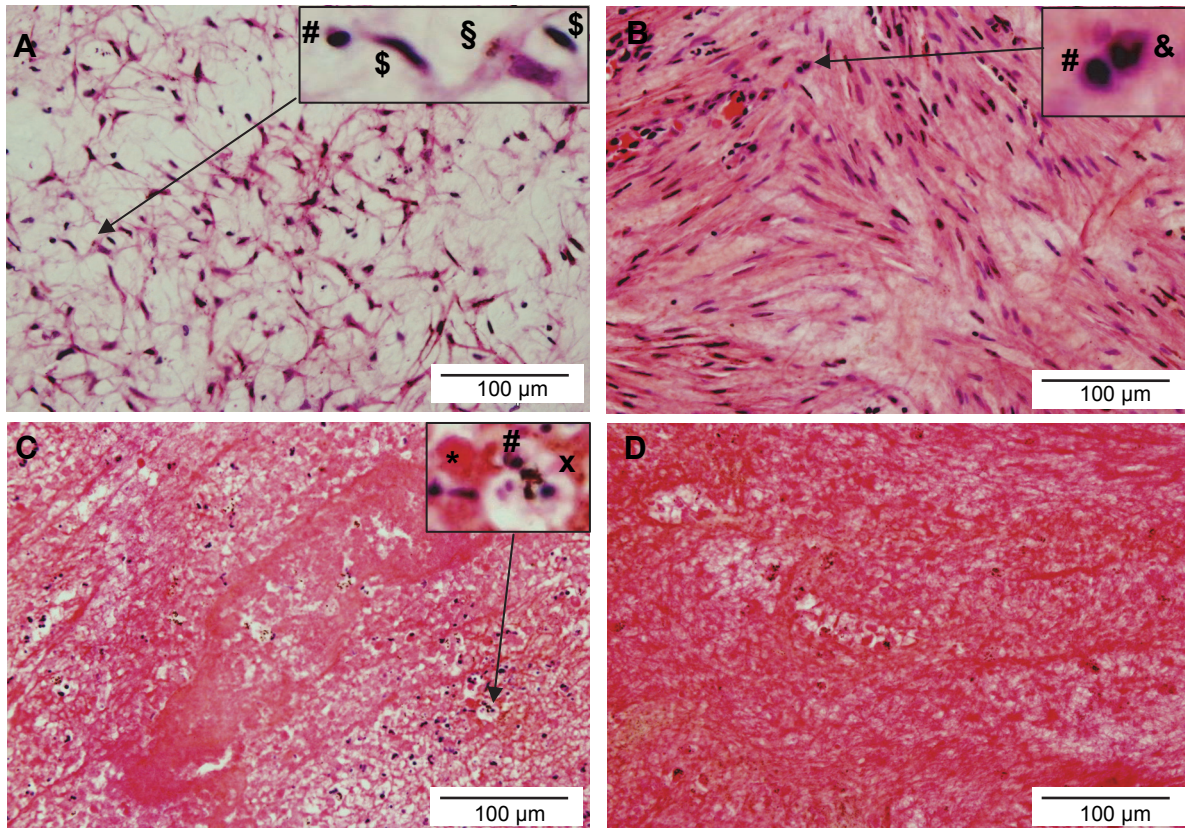


**Fig.4: HE staining of PEA tissues.**

(A) Representative image from distal area of the PEA tissue showing loose connective tissue, fibrocytes (\$) and fibroblasts (§) as well as lymphocytes (#). (B) Representative image from the distal area of PEA material with loose connective tissue, lymphocytes (#) and eosinophils (&). (C) Sample from the proximal tissue shows high number of neutrophils, erythrocytes (\*) and low number of lymphocytes as well as macrophages (x) (D).

The distal areas of the PEA tissue show predominantly the presence of fibroblasts and fibrocytes, whereas the proximal areas are mainly rich in erythrocytes. In both areas the presence of lymphocytes and eosinophils could be observed (Fig.4).

Further examining the HE stainings of the distal and central PEA tissues from different patients, it can be observed that the distal pieces (n=12) tend to have a higher percentage of eosinophils compared to the central pieces (n=19). Macrophages, lymphocytes, fibroblasts and neutrophils are equally distributed in both tissue areas, whereas vessels are mainly detected in the distal PEA tissues (Table 2, Fig.5). The interpretation of HE analysis should be taken with precaution, due to the very small pool of patients used for analysis.

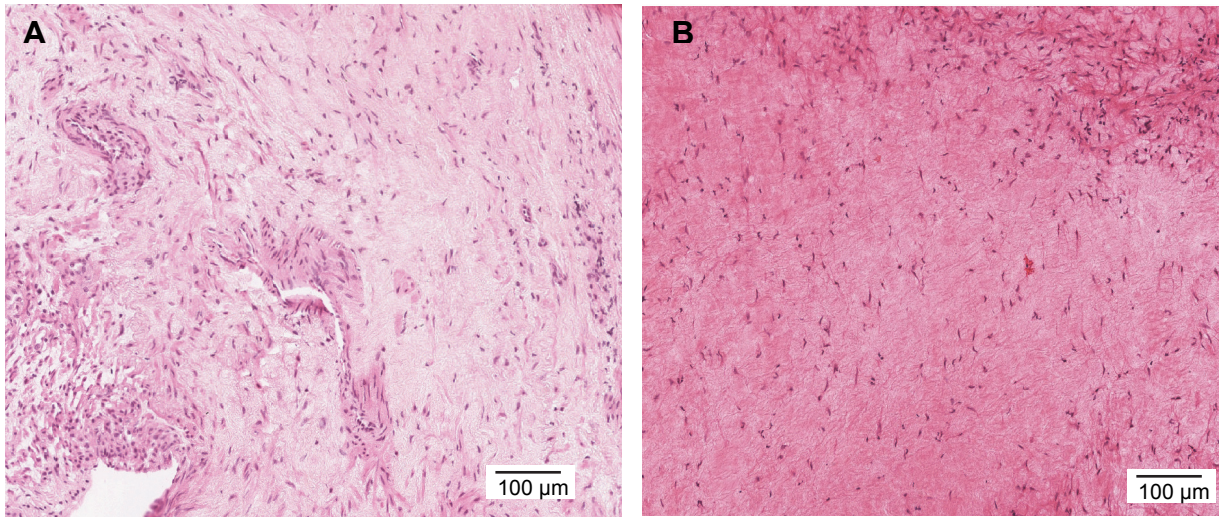


**Fig.5: HE staining of PEA tissues.**

(A) Representative image from distal area of collected PEA tissues showing loose connective tissue, fibrocytes and fibroblasts as well as vessels and eosinophils in the distal parts. (B) Representative image from the central area of PEA material.

**Table 2: HE analysis of tissue slides (number of slides/%)**

	erythrocyte		neutrophil		lymphocyte		macrophage	
	Central	distal	central	distal	central	distal	central	distal
<b>0</b>	2/10,53	2/16,67	3/15,79	0/0,00	1/5,26	0/0,00	0/0,00	1/8,33
<b>I</b>	10/52,63	5/41,67	15/78,95	11/91,67	16/84,21	8/66,67	12/63,16	8/66,67
<b>II</b>	5/26,32	4/33,33	1/5,26	1/8,33	2/10,53	4/33,33	6/31,58	3/25,00
<b>III</b>	2/10,53	1/8,33	0/0,00	0/0,00	0/0,00	0/0,00	1/5,26	0/0,00
<b>total</b>	<b>19</b>	<b>12</b>	<b>19</b>	<b>12</b>	<b>19</b>	<b>12</b>	<b>19</b>	<b>12</b>

	collagen		fibrocytes		vessels		eosinophils	
	central	distal	central	distal	central	distal	central	distal
<b>0</b>	7/36,84	2/16,67	7/36,84	2/16,67	13/68,42	4/33,33	14/73,68	2/16,67
<b>I</b>	9/47,37	7/58,33	6/31,58	3/25,00	6/31,58	6/50,00	5/26,32	10/83,33
<b>II</b>	3/15,79	3/25,00	6/31,58	6/50,00	0/0,00	2/16,67	0/0,00	0/0,00
<b>III</b>	0/0,00	0/0,00	0/0,00	1/8,33	0/0,00	0/0,00	0/0,00	0/0,00
<b>total</b>	<b>19</b>	<b>12</b>	<b>19</b>	<b>12</b>	<b>19</b>	<b>12</b>	<b>19</b>	<b>12</b>

## Vessels are present in PEA surgical material of CTEPH patients

Depending on disease grade, the thrombotic clot is organized in a certain stage. This leads to the formation of vessels (black arrows). On one hand, endothelial cells (vWF positive) surrounded by smooth muscle cells (sm $\alpha$ -actin positive) are visible forming muscularized vessels (Fig.6B) on the other hand newly developed vessels or arteriole-like vessels with only one layer of endothelial cells (CD31 positive; Fig.6A) are observed. The vessel formation in the PEA tissue could be mainly observed in the distal areas of the clots. There 67% of the analyzed slides had vessels present, whereas 68% of the central parts lacked vessels (Table 2).

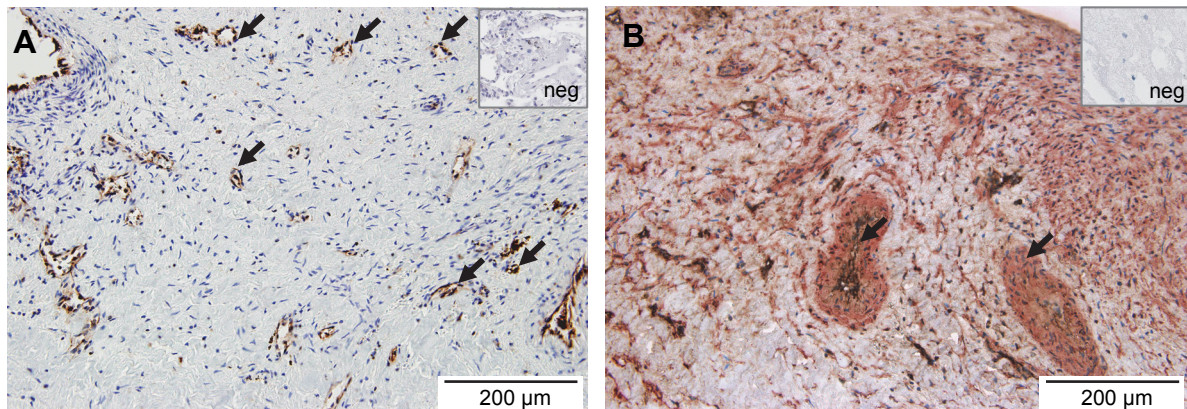


**Fig.6: Paraffin-embedded PEA tissues.**

(A) CD31 positive endothelial cells (brown) in distal PEA samples. (B) Double staining for von Willebrand factor (brown) and smooth muscle  $\alpha$ -actin (red) shows muscularized vessels (black arrows). The nuclei are counterstained with Haemalaun (blue). Negative control is shown as inset (neg).

In summary, we could show the characteristic appearance of the PEA material taken from CTEPH patients, which consists of inflammatory cells such as macrophages and lymphocytes, structural cells for example fibroblast and fibrocytes as well as vascular cells (endothelial and smooth muscle cells), forming partial recanalization in the clot.

## **PART 2**

---

### **Isolation and characterization of CTEPH-hECs**

To investigate the endothelial cells of the CTEPH patients (CTEPH-hECs), the cells outgrowing from the tissue were cultured under standard conditions. At early stage of isolation a mixed culture of cells was achieved (Fig.7A), which were further sorted via CD31 labelled magnetic beads. To examine the phenotype of the received culture, the CTEPH-hECs were stained for vWF and VE-cadherin (Fig.7B, D). A further tool for characterization is the negativity of the cells for smooth muscle  $\alpha$ -actin (Fig.7C).

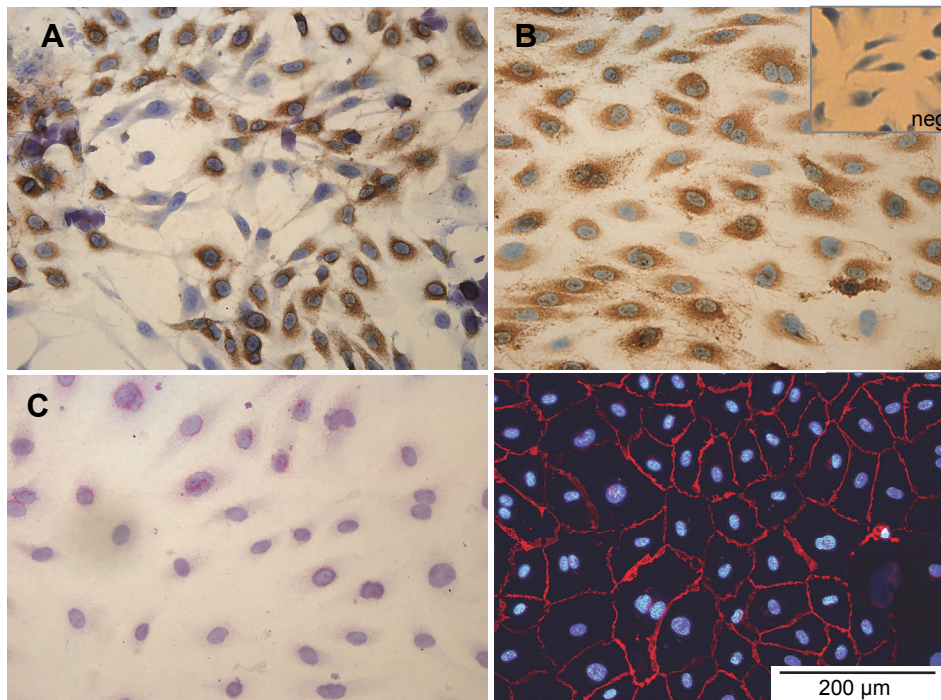


**Fig.7: Isolation and characterization of endothelial cells from PEA tissue.**

(A) Mixed culture of cells growing out from the PEA tissue. Significant proportion of cells show vWF positive signal (brown). (B) Pure, vWF (brown) positive endothelial culture after CD31 magnetic bead sorting. (C) Lack of the staining for smooth muscle  $\alpha$ -actin in the CD31-sorted CTEPH-hEC population. (D) CTEPH-hECs form tight monolayer with intense VE-cadherin (red) staining. Nuclei are counterstained blue with DAPI. Negative control is shown as inset.

Normally, if the clots do not dissolve by themselves, a high amount of newly formed vessels develop in the clot of venous emboli to recanalize the occluded area (57-59). In contrast, this does not happen in CTEPH patients, or only at a very small degree. Therefore the question arises, whether the vessel forming ability of CTEPH-hECs is affected/alterd. Therefore an angiogenesis test was performed, where the vessel forming ability of the cells isolated from PEA was compared with healthy hPAECs. The results show, that after 21h there was no difference in the vessel formation of CTEPH-hECs as compared to hPAECs (Fig.8A, B) ( $p = 0,60$ ).

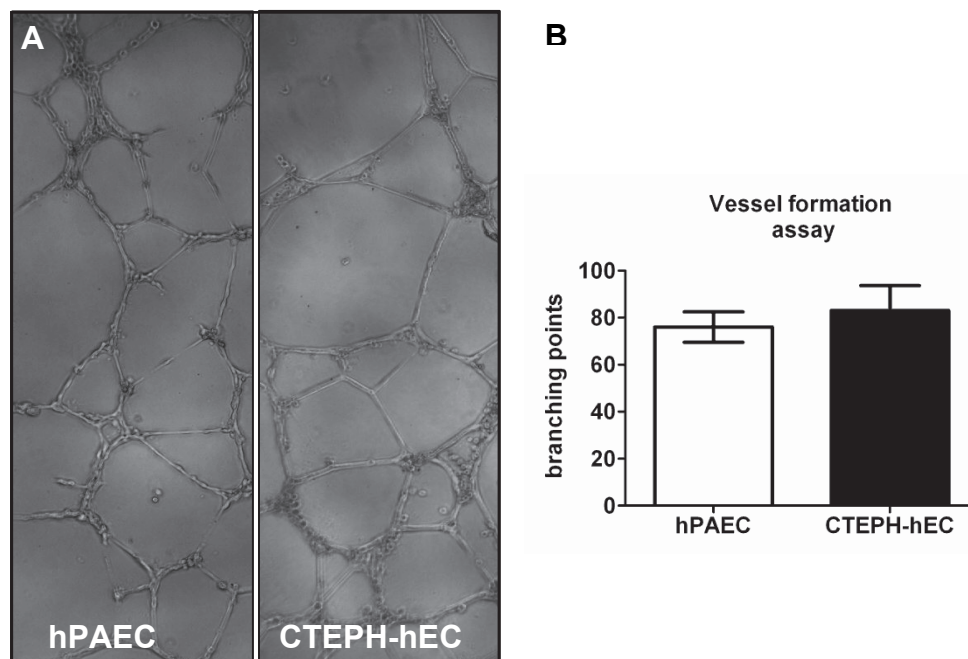


**Fig.8: Vessel formation of endothelial cells from PEA tissue.**

(A) Representative pictures of vessel formation on Matrigel after 21h of hPAECs and CTEPH-hECs. (B) Bar graph shows summarized results of vessel formation assay as number of branching points (hPAEC:  $76 \pm 6,42$  %; CTEPH-hEC:  $83 \pm 10,60$  %;  $n_{exp}=3$ ).

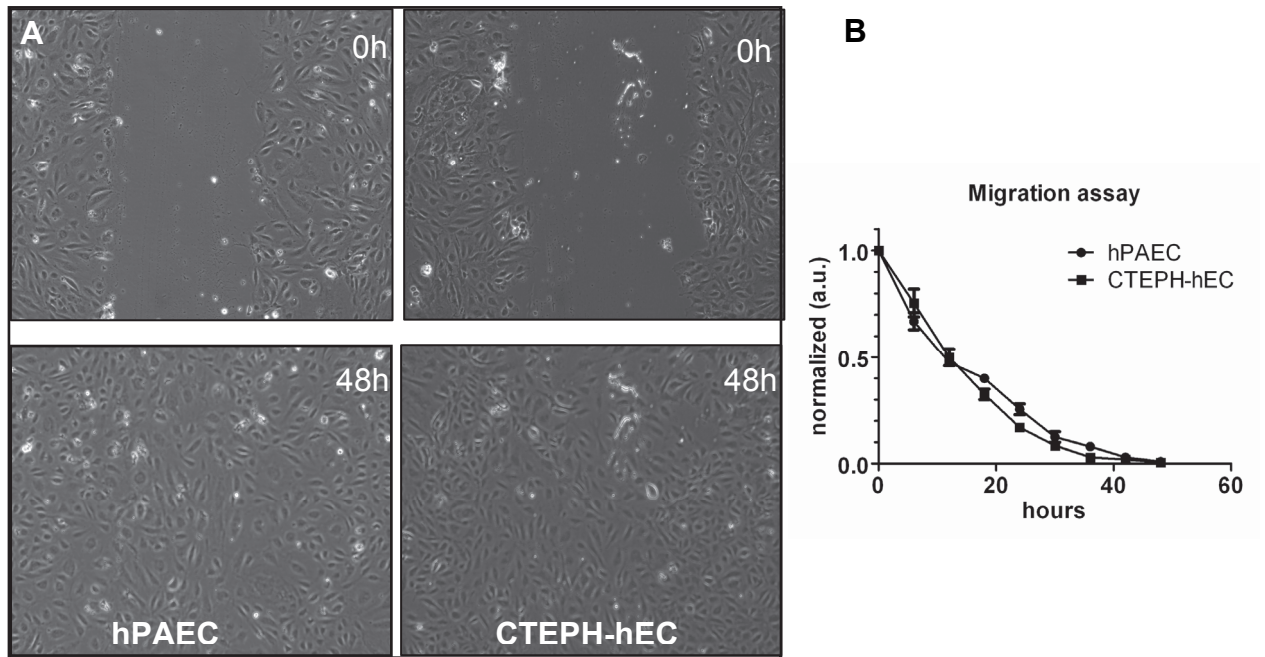


**Fig.9: Migration ability of endothelial cells from PEA tissue.**

(A) Representative images of migration assay of CTEPH-hECs and hPAECs. (B) Graph shows normalized results of the migration assay as decrease in cell free area ( $n_{exp}=3$ ).

To check the migration abilities of CTEPH-hECs a wound healing assay was performed. The results show that the CTEPH-hECs have the same degree of wound closure as healthy hPAECs over 48h (Fig.9A, B). Although the CTEPH-hECs behave in general like hPAECs, they showed a significant increase in proliferation (Fig.10).

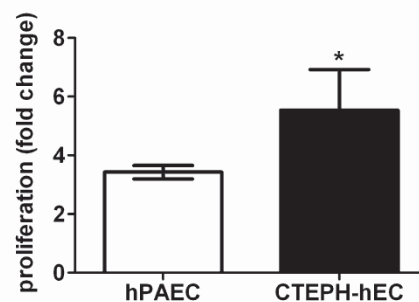


**Fig.10: Proliferation of endothelial cells from PEA tissue.**

Proliferation of the CTEPH-hECs and control human pulmonary artery endothelial cells (hPAECs) in culture for 4 and 8 days. The graph represents the fold change in the cell number from day 4 to 8 ( $n_{exp}=4$ ;  $n_{patients}=3$ ); (\* =  $p<0,05$ ).

To further investigate the reason for the increased proliferation, we decided to look at the  $\text{Ca}^{2+}$  homeostasis of the CTEPH-hECs and compare them with hPAECs (Fig.11, 12). The CTEPH-hECs showed a significant increase in the basal intracellular calcium level compared to hPAECs (Fig.11B). By treating both cell types with different stimuli (histamine, BHQ), the CTEPH-hECs responded with a higher increase in intracellular  $\text{Ca}^{2+}$  compared to hPAECs. First the effect of histamine was investigated in detail. 10 $\mu\text{M}$  histamine led to a significant higher histamine induced calcium increase in the CTEPH-hECs (compared to hPAECs as shown in Fig.11C).

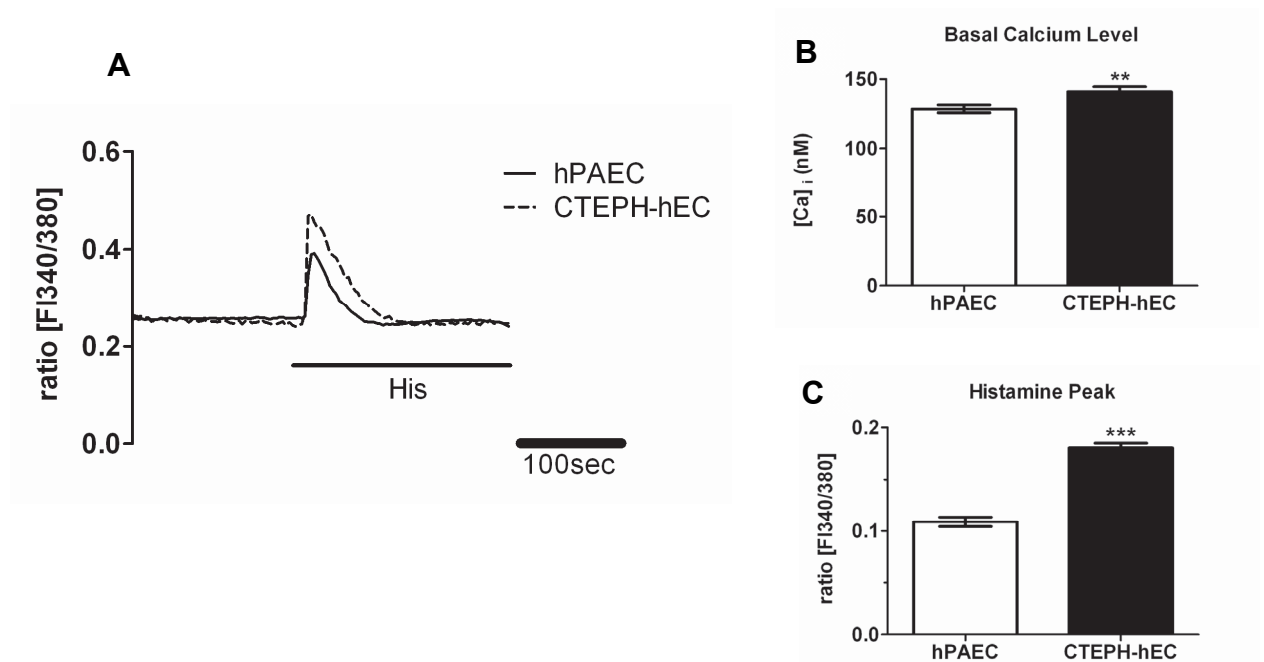


**Fig.11: Calcium homeostasis of CTEPH-hECs and hPAECs.**

(A) Representative graph of the histamine-induced increase in the intracellular calcium concentration. (B) Bar graphs showing the basal calcium level of CTEPH-hECs and hPAECs. (C) Summarized results of the histamine induced peak height in CTEPH-hECs and hPAECs; (\*\*  $p < 0,01$ , \*\*\*  $p < 0,001$  compared to control).

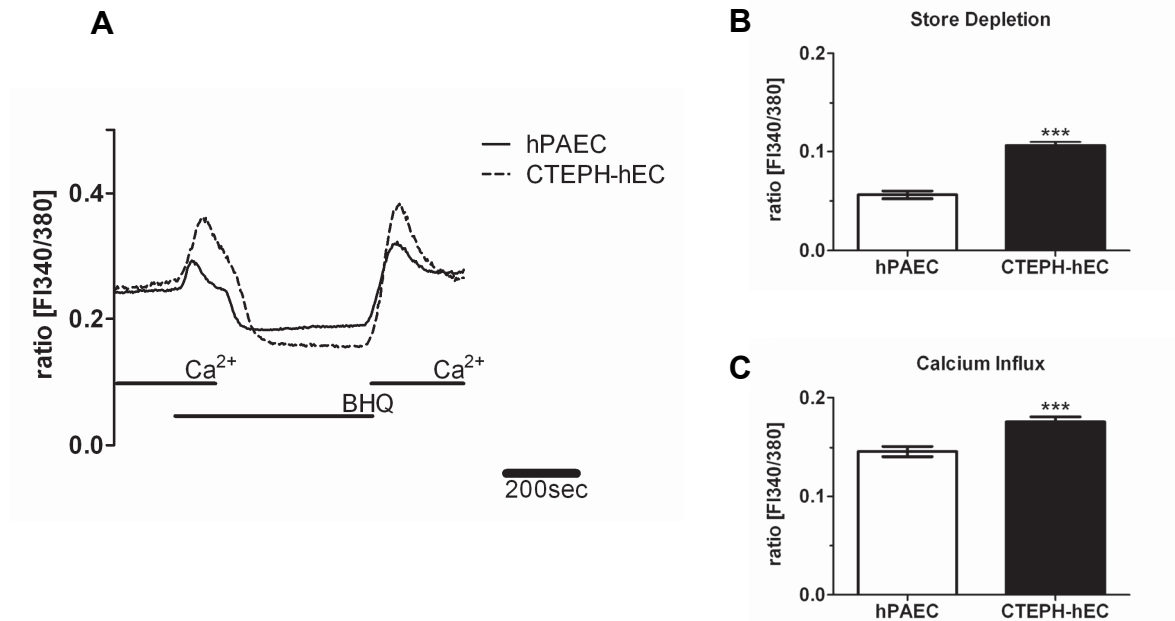


**Fig.12: Calcium homeostasis of CTEPH-hECs and hPAECs.**

(A) Representative recording of the calcium store depletion. (B) Summarized data of the store depletion (measured as the peak of the calcium release) in CTEPH-hECs in comparison to hPAECs. (C) The mean amplitude of the changes in the intracellular Ca<sup>2+</sup> signal when external calcium was readmitted to the CTEPH-hECs and hPAECs; (\*\*\*)  $p < 0,001$  compared to control).

**Table 3: Calcium parameters of hPAECs vs CTEPH-hECs (\*\*  $p < 0,01$  , \*\*\*  $p < 0,001$ )**

	hPAECs	CTEPH-hECs
<b>Basal Calcium Level (nM)</b>	129±3 (n=518)	141±4 ** (n=433)
<b>Histamine Peak (Δratio)</b>	0.11±0.01 (n=213)	0.18±0.01 *** (n=215)
<b>Store Depletion (Δratio)</b>	0.06±0.004 (n=201)	0.11±0.004 *** (n=275)
<b>Calcium Influx (Δratio)</b>	0.15±0.01 (n=218)	0.18±0.01 *** (n=302)

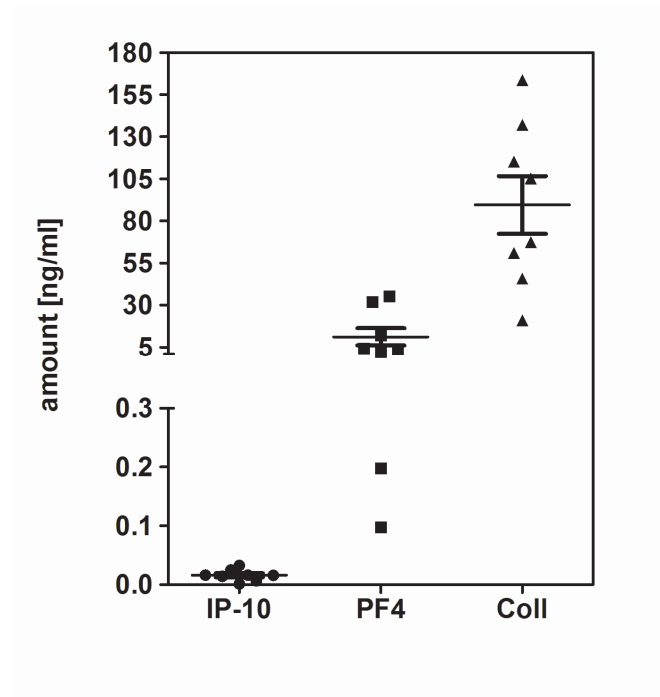
Looking at the store depletion and Ca<sup>2+</sup> influx, in both cases CTEPH-hECs showed a significant increase in the intracellular Ca<sup>2+</sup> levels when comparing to hPAECs ( $p$ -value<0,0001); (Fig.12 B, C; Table 3).

Taken together, CTEPH-hECs behave similarly as typical arterial ECs. They show similar properties with respect to surface markers (vWF; VE-cadherin), their migratory behaviour and vessel formation ability. But they show a significant increase in proliferation, which could be explained with the significant basal calcium level increase. Moreover, the CTEPH-hECs show a difference in their  $\text{Ca}^{2+}$  homeostasis, due to increased cytosolic  $\text{Ca}^{2+}$  mobilization upon histamine or BHQ stimuli as well as increased store operated calcium entry compared to hPAECs.

## PART 3

### Angiostatic factors present in the PEA tissue influence calcium homeostasis

The pulmonary arteries of the CTEPH patients are occluded over years. However, a total recanalization, which would lead to a regained blood flow in the lung, does not occur in the thrombi. Other factors in the microenvironment of the vessel forming cells present in the clot might disturb or retard angiogenesis. To test this hypothesis the presence of angiostatic factors were checked on protein level via ELISA and indeed IP-10, PF4 (CXCL4) and collagen type I could be detected in various amount in the supernatant of the PEA tissue (Fig.13) as well as at tissue level (Fig.14A, B, C).



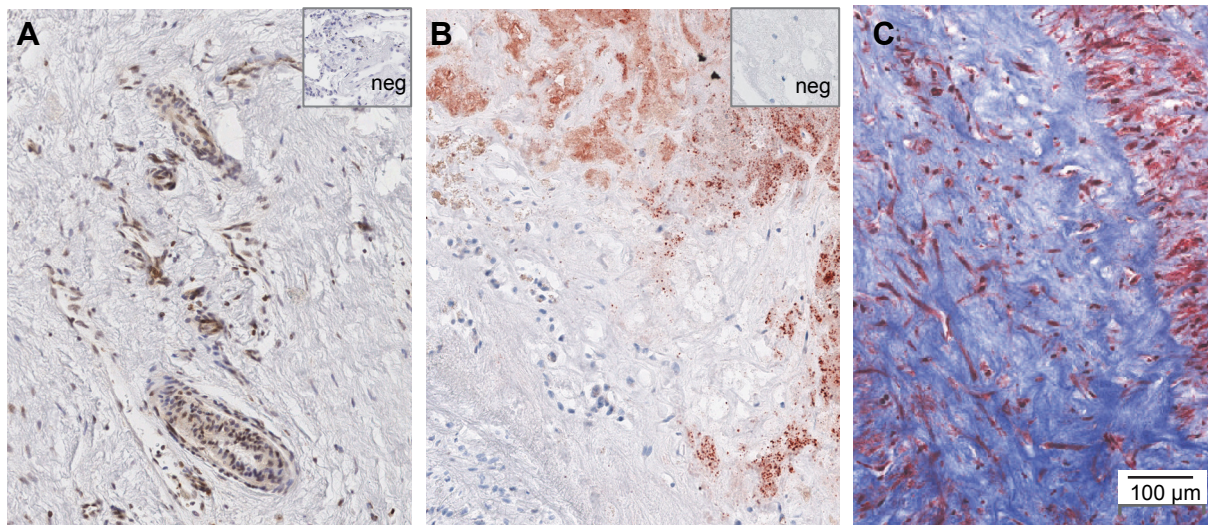


**Fig.14: IP-10, PF4 and collagen in PEA tissue.**

Immunohistochemical stainings for IP-10 (A), PF4 (B) and trichrome staining (C). Negative control shown as inset (neg).

Beside the ligands IP-10 and PF4, also their receptor (CXCR3) was present in PEA tissue and human lungs. CXCR3 was detectable in the endothelial cells as well as in a certain degree in surrounding SMCs and fibroblasts (Fig.15A, B). CXCR3 mRNA was detected in mRNA of isolated CTEPH-hECs as well as in hPAECs of three different donors (Fig.16).

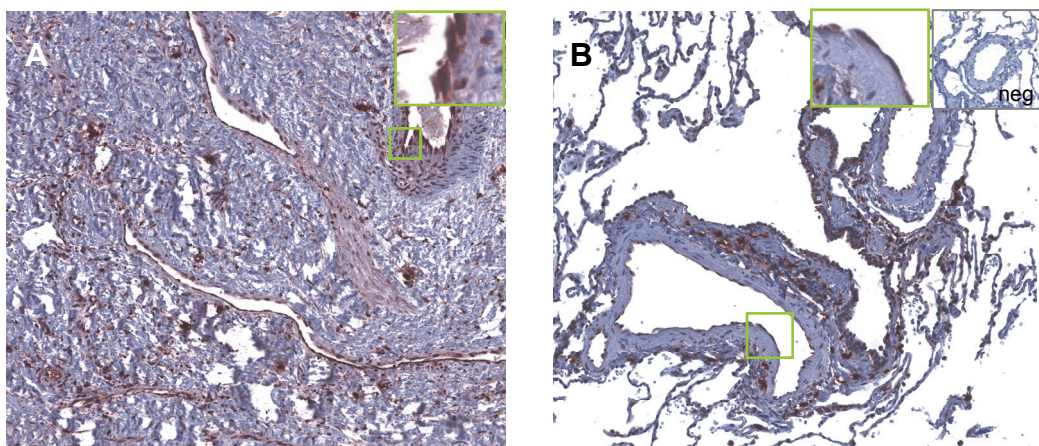


**Fig.15: IP-10 and PF4 receptor CXCR3 in PEA tissue and human lung.**

(A) Immunohistochemical staining on paraffin embedded tissue from CTEPH patients for CXCR3 (20X). CXCR3 staining localized mainly in the vessel forming endothelial cells, in the surrounding smooth muscle cells and fibroblasts. (B) Human lung tissue from a healthy control stained for CXCR3 (20X). Inset shows magnification of the green box region. Negative control shown as inset (neg).

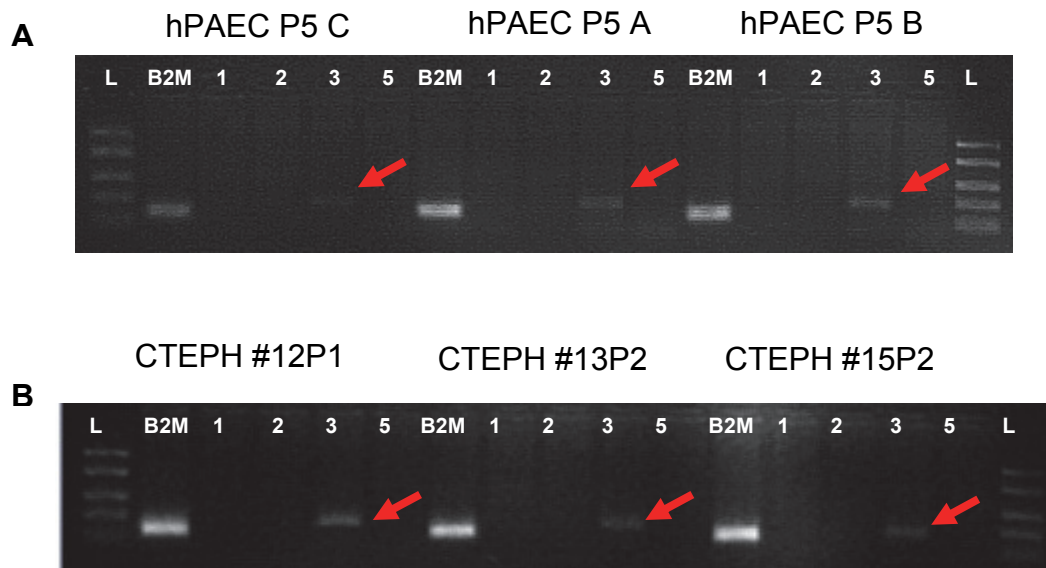


**Fig.16: Expression of CXCR3 in PEA tissue and human lung.**

Expression of CXCR3 at mRNA level in hPAECs (A) and CTEPH-hECs (B) from 3 different patients ( $p$ = passage number). The expression of CXCR1, 2 and 5 were not detectable (A and B column 1, 2, 5) As an internal control Beta-2 microglubulin (B2M) was used.

To have a closer look at the expression pattern of CXCR3, RT-PCR was performed and the expression present in PEA tissue was compared to the expression pattern in healthy human lung tissue (Fig.17). CXCR3 in the distal PEA tissue is up-regulated compared to the healthy lung tissue, whereas in the central part the CXCR3 expression is not changed. Therefore it can be stated, that CXCR3 is in a higher degree present in the distal PEA tissue compared to the central one. Looking at the total (central and distal combined) CXCR3 expression in PEA tissue, CXCR3 is more expressed in the PEA tissue compared to the human lung ( $1,5\pm0,53$  fold).

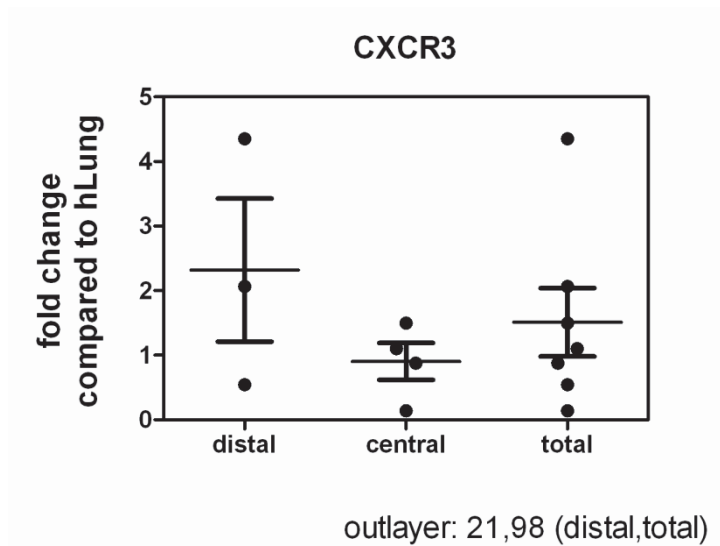


**Fig.17: RT-PCR expression of CXCR3 in PEA tissue and human lung.**

Relative expression of CXCR3 in distal, central respectively total PEA tissue compared to human lung.

Due to the presence of the above mentioned three factors (IP-10, PF4 and collagen type I) in the PEA tissue we addressed the question of their effect on the calcium homeostasis of hPAECs (Fig.18). The basal calcium level, store depletion and the calcium influx of hPAECs treated for 6h or 24h with IP-10 (600ng/ml), PF4 (400ng/ml) or Collagen type I (100µg/ml) were measured (Table 4-6). In case of 6h IP-10 treatment the basal calcium level showed no significant difference compared to control cells, whereas 24h IP-10 treatment increased the EC basal calcium level (Fig.18B). Looking at the store depletion no difference between control and 6h or 24h IP-10 treated cells could be observed (Fig.18C). Interestingly a significant increase in calcium influx in as well as 24h IP-10 stimulated cells could be seen compared to control cells (Fig.18D). Looking at the basal calcium changes in PF4 stimulated cells neither 6h nor 24h led to a significant increase compared to control cells (Fig.18E). In line with the IP-10 stimulated cells 6h PF4 treatments led to no change compared to control cells, whereas the 24h PF4 treatment showed a significant increase in calcium store depletion (Fig.18F). Store operated calcium entry increased only in 24h but not in 6h PF4 treated cells compared to control (Fig.18G). In case of collagen treatment we observed a significant elevation in basal calcium compared to untreated cells (Fig.18H). Looking at the store depletion of the collagen treated cells a significant increase compared to the control cells could be detected (Fig.18I). A significant

elevated calcium influx, like in the case of IP-10 and PF4 treatment, was also observed in the 6h collagen treated cells compared to the controls (Fig.18J).

**Table 4: Calcium parameters of hPAECs upon IP-10 stimuli**

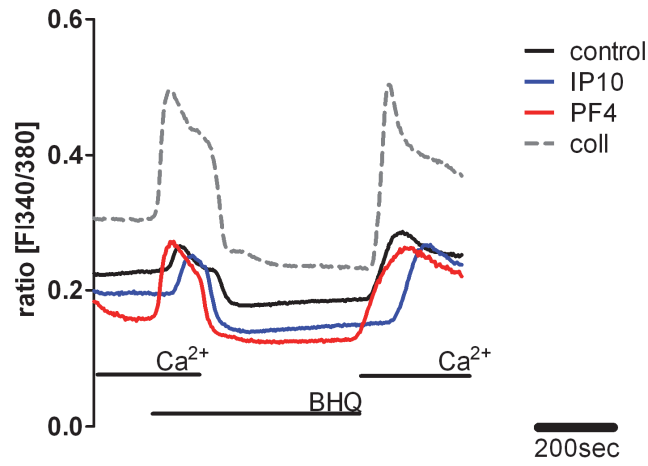
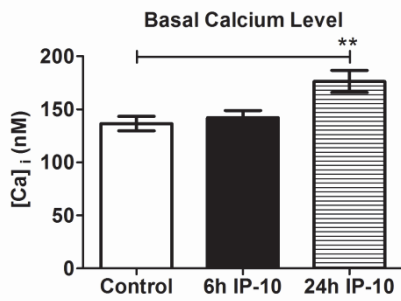
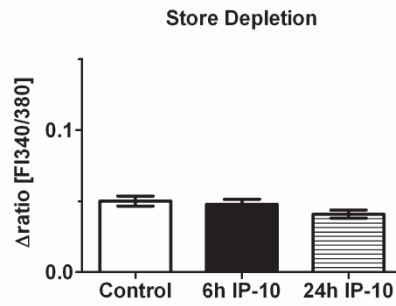
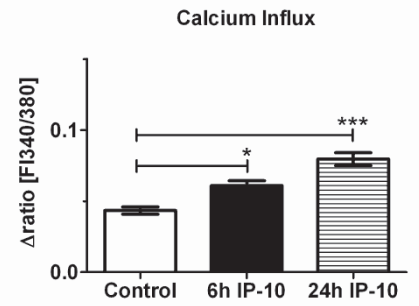
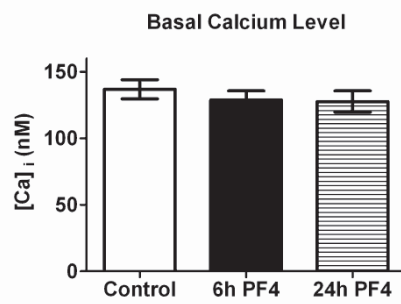
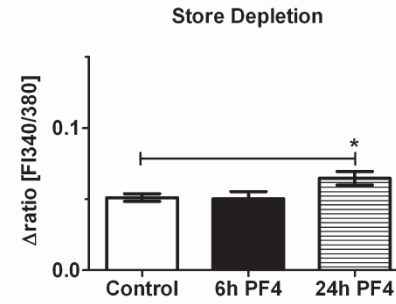
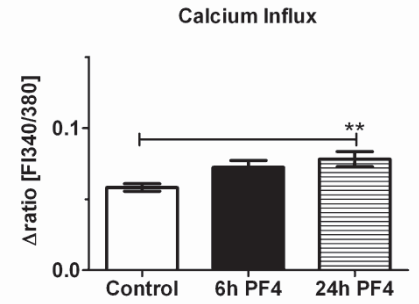
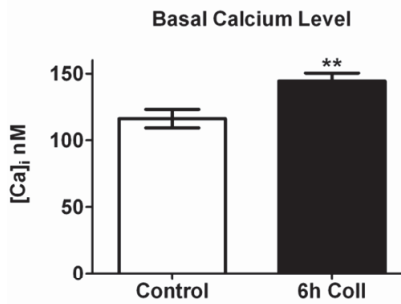
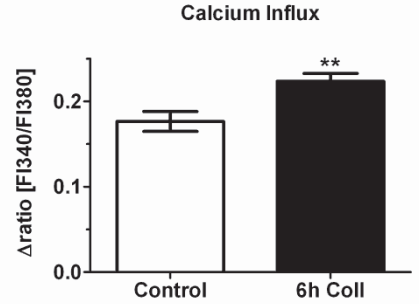
	<b>control</b>	<b>6h IP-10</b>	<b>24h IP-10</b>
<b>Basal Calcium Level (nM)</b>	137 ± 7 (n=67)	142 ± 7 (n=47)	176 ± 10 ** (n=43)
<b>Store Depletion (Δratio)</b>	0.05 ± 0.004 (n=47)	0.05 ± 0.004 (n=47)	0.04 ± 0.003 (n=78)
<b>Calcium Influx (Δratio)</b>	0.04 ± 0.003 (n=42)	0.06 ± 0.003 * (n=47)	0.08 ± 0.01 *** (n=77)

**Table 5: Calcium parameters of hPAECs upon PF4 stimuli**

	<b>control</b>	<b>6h PF4</b>	<b>24h PF4</b>
<b>Basal Calcium Level (nM)</b>	137 ± 7 (n=63)	129 ± 7 (n=52)	128 ± 8 (n=52)
<b>Store depletion (Δratio)</b>	0.05 ± 0.003 (n=112)	0.05 ± 0.01 (n=52)	0.06 ± 0.01* (n=83)
<b>Calcium influx (Δratio)</b>	0.06 ± 0.003 (n=98)	0.07 ± 0.01 (n=51)	0.08 ± 0.01** (n=83)

**Table 6: Calcium parameters of hPAECs upon collagen stimuli**

	<b>control</b>	<b>6h Coll</b>
<b>Basal Calcium Level (nM)</b>	116 ± 7 (n=40)	145 ± 6** (n=35)
<b>Store depletion (Δratio)</b>	0.06 ± 0.01 (n=57)	0.14 ± 0.01*** (n=69)
<b>Calcium influx (Δratio)</b>	0.18 ± 0.01 (n=57)	0.22 ± 0.01** (n=69)

**A****B****C****D****E****F****G****H****I****J**

**Fig.18: Effect of IP-10, PF4 and collagen type I on hPAEC calcium homeostasis.**

(A) Representative recording of the Ca<sup>2+</sup> store depletion. (B) Bar graphs show the basal Ca<sup>2+</sup> level of untreated (control), 6h and 24h IP-10 treated hPAECs. (C) Summarized data of the 6h IP-10 and 24h IP-10 treatment on store depletion compared to untreated hPAECs (control). (D) Effect of 6h IP-10 treatment and 24h IP-10 treatment on Ca<sup>2+</sup>influx compared to control. Bar graphs showing the basal Ca<sup>2+</sup> level of untreated (control), and 6h or 24h PF4 treated hPAECs (E). (F) Summarized data of the PF4 treatment effect after 6h and 24h on store depletion (measured as the peak of the Ca<sup>2+</sup> release) compared to control. (G) Mean amplitude of the Ca<sup>2+</sup> signal when external calcium was readmitted on control and 6h or 24h PF4 treated hPAECs. (H) Bar graphs show the basal Ca<sup>2+</sup> level of untreated (control) and collagen type I treated hPAECs. (I) Summarized data of the collagen type I treatment on store depletion compared to untreated hPAECs (control). (J) Effect of collagen type I treatment on Ca<sup>2+</sup> influx compared to control (\*p<0.05, \*\* p<0.01, \*\*\* p<0.001 compared to control untreated cells).

## Angiostatic factors from the PEA tissue lead to endothelial dysfunction.

The angiostatic effect of IP-10 and PF4 is well known (60-62). To investigate the angiostatic effect of IP-10, PF4 and collagen type I migration (wound closure), proliferation and vessel formation was tested. An important mechanism in vessel formation is the migration of ECs, therefore a migration assay with periodic recordings of the wound healing was performed (Fig.19A, B).

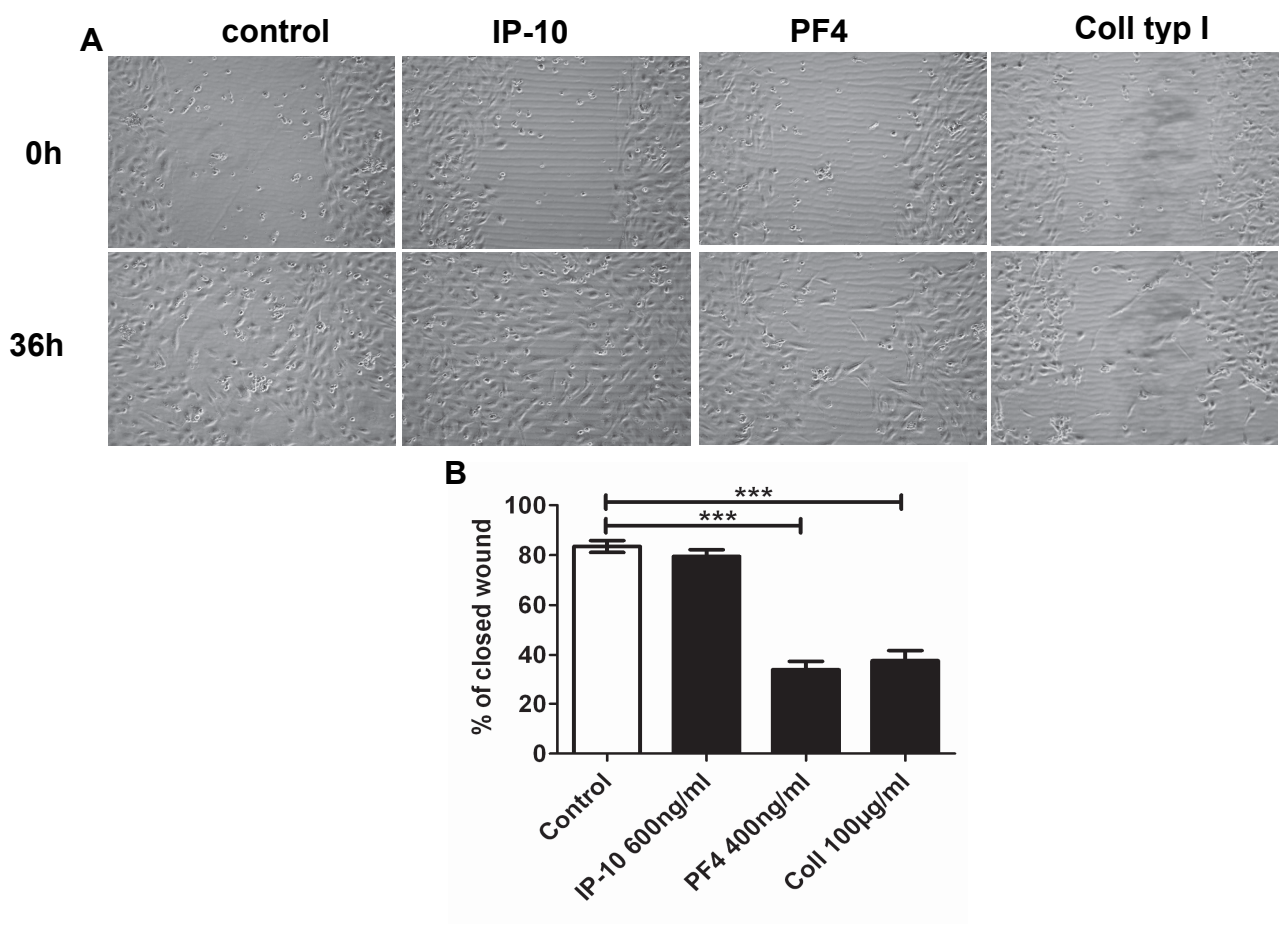


**Fig.19: Effect of IP-10, PF4 and collagen on hPAECs wound healing.**

(A) Representative images of migration assay showing the effect of IP-10 (600ng/ml), PF4 (400ng/ml) and collagen type I (100µg/ml) on hPAECs. (B) Summarized results of wound healing after 36h (n=3); (\*\*\*)  $p < 0,001$  compared to control).

The bars on Fig.19B show that in case of control the cells were able to close the wound up to  $83,53 \pm 2,38$  % within 36h. In contrast, cells under PF4 treatment were only able to close the wound up to  $34,10 \pm 3,37$  % and under Collagen type I treatment up to  $37,57 \pm 4,08$  %, showing a significant delay of wound closure in both cases compared to control. Interestingly, IP-10 ( $79,57 \pm 2,59$  %) did not show significant difference in migration as compared to control (Fig.19A, B) and moreover induced proliferation (Fig.20).

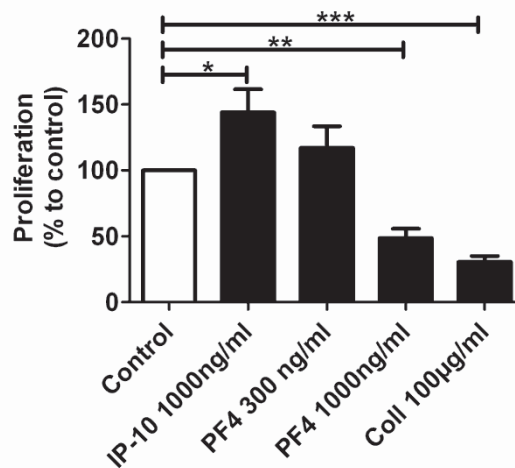


**Fig.20: Effect of IP-10, PF4 and collagen on hPAECs proliferation.** Bar graph summarizing the effect of different factors on hPAECs proliferation compared to untreated hPAECs. (\*  $p < 0,05$  ; \*\*  $p < 0,01$  ; \*\*\*  $p < 0,001$  compared to control)

In case of proliferation, which also plays an important role in vessel formation, PF4 with 1000ng/ml and collagen type I (100µg/ml) were able to significantly decrease the proliferation of hPAECs up to 42% and 64% compared to non-treated cells (Fig.20).

Beside wound closure and proliferation, chemotaxis is important in migration of the ECs to the place where they form vessels. Therefore the chemotactic ability of IP-10, PF4 and collagen type I was assessed resulting in no change in EC behaviour upon 5h treatment (Fig.21A, B). The % of migrated cells compared to control did not change IP-10, PF4 or collagen type I treatment could be observed (Fig.21B).

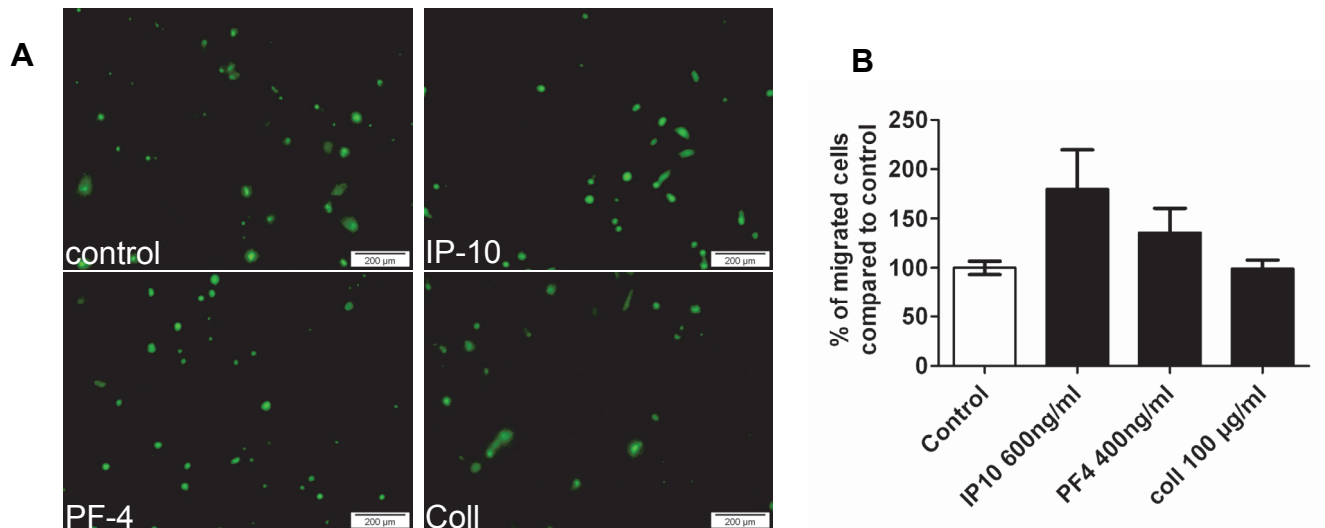


**Fig.21: Effect of IP-10, PF4 and collagen on hPAECs migration.**

(A) Representative fluorescent images of migrated hPAECs under different treatment. (B) The bars show the % of cells compared to control, which migrated to the bottom of the filter within 5h.

To assess the permeability change of the hPAECs monolayer upon IP-10, PF4 or collagen type I treatment, a permeability assay was applied. Only 6h collagen type I treatment showed a significant increase in permeability (Fig. 22C), whereas IP-10 and PF4 had no effect (Fig.22A and B).

The increase in permeability in case of collagen type I treatment was due to a cell-cell contact detachment, which could be validated by looking at the cell-cell contact protein VE-cadherin. By treating the hPAECs for 6h with collagen type I a decrease in VE-cadherin staining could be observed (Fig.22E).

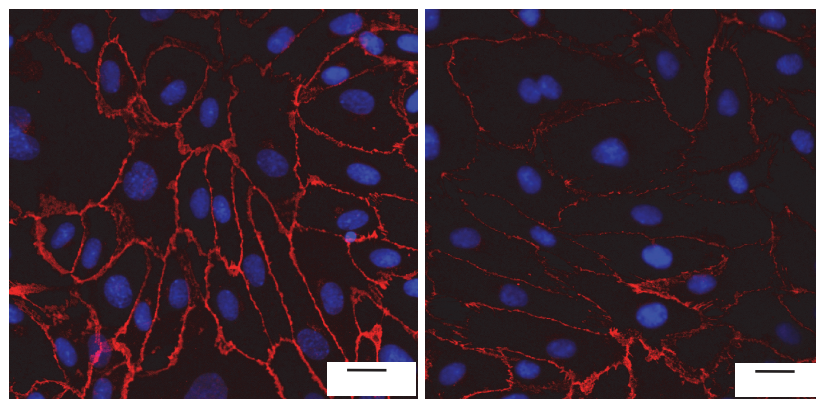
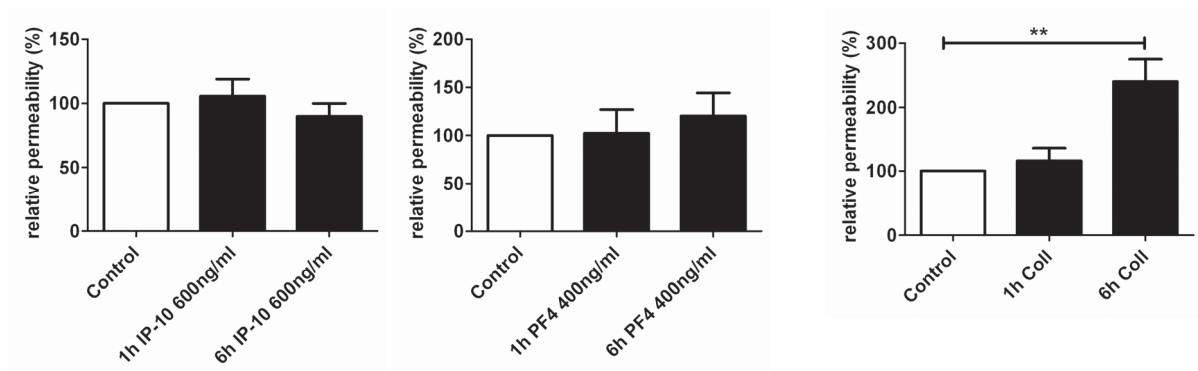


**Fig.22: Effect of IP-10, PF4 and collagen type I on hPAECs permeability.**

Bar graphs summarising the effect of (A) IP-10 (600ng/ml), (B) PF4 (400ng/ml) and (C) Collagen type I (100µg/ml) after 1h and 6h treatment on hPAEC permeability. (\*\* $p < 0,01$  compared to control). Effect of 6h (E) collagen type I on VE-cadherin expression in hPAECs compared to control (D).

As a next step the effect of the three factors (IP-10, PF4 and collagen) on vessel formation was tested. For this reason an *in vitro* angiogenesis assay was applied (Fig.23A, B). The graph represents a number of loops formed on matrigel. In this case the cells treated with IP10, PF4 and Collagen type I, showed a significant decrease of number of loops formed within 6h compared to control. The strongest effect could be observed in the collagen treated hPAECs, there a 64,82% decrease in number of loops compared to control could be observed. PF4 lead only to a 41,21% decrease, whereas the weakest effect could be achieved with IP-10 treatment (24,14%).

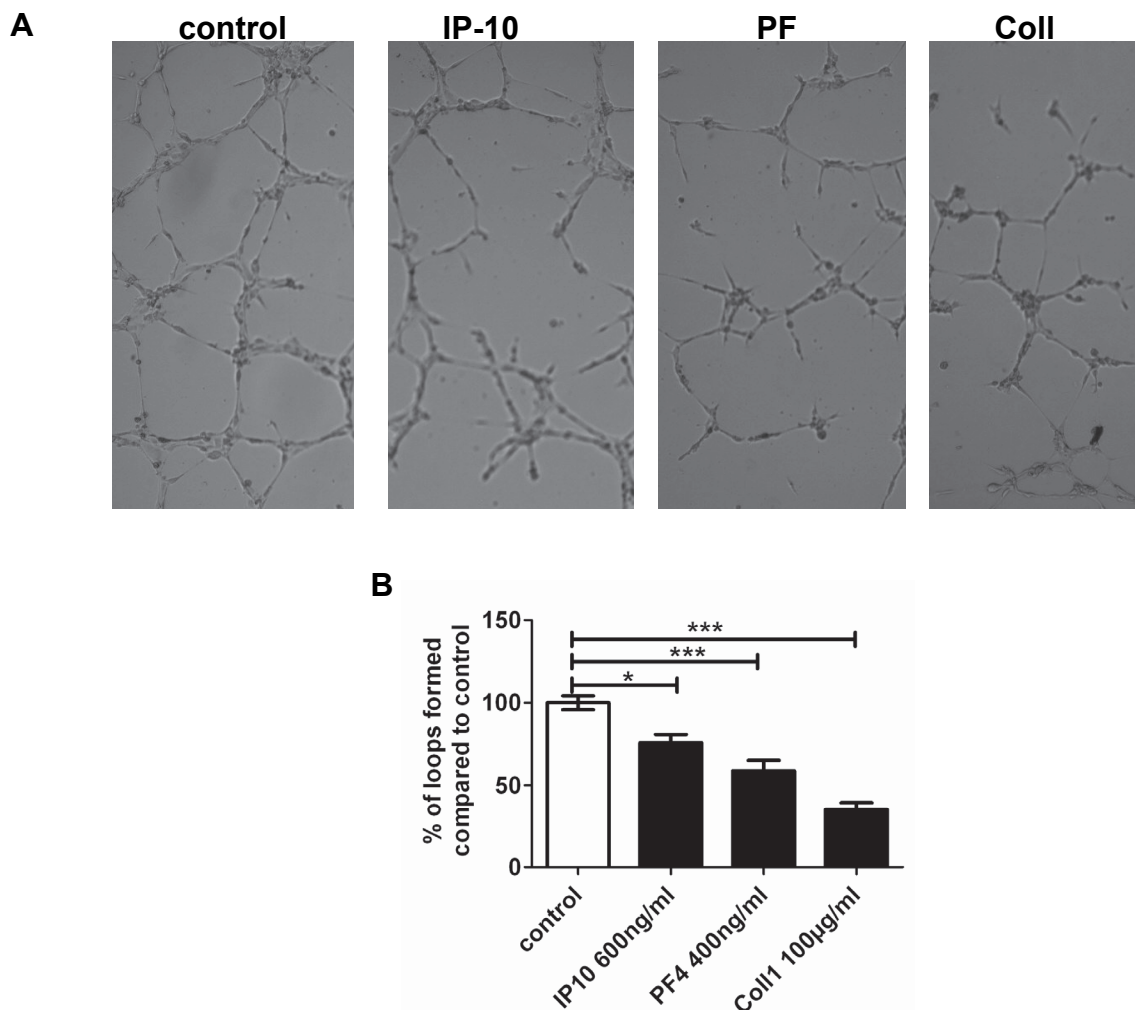


**Fig.23: Effect of IP-10, PF4 and collagen on hPAECs vessel formation.**

(A) Representative image (4X) of vessels formed after 6h under different stimuli. (B) Bar graph presenting the % of formed loops compared to control (\*  $p < 0,05$ , \*\*\*  $p < 0,001$  compared to control).

In summary we could detect three factors PF4, IP-10 and collagen type I in the supernatant of the PEA tissue as well as at tissue level. Challenging healthy control cells (hPAECs) with these factors for either 6h or 24h led to a significant change in the calcium homeostasis. In addition PF4 and collagen type I led to a significant decrease in proliferation, wound healing and vessel formation, whereas IP-10 just decreased the vessel formation ability and interestingly increased the proliferation of the hPAECs. Chemotaxis was not altered upon stimulation with these three factors. These results indicate that the three factors found in the microenvironment of the clot alter EC function, leading to a disturbed or retarded angiogenesis and therefore are able to delay the recanalization process of the clot.

## PART 4

### Presence of inflammatory factors in CTEPH-tissue

The role of other factors present in the microenvironment of the PEA tissue deserves further investigations. Therefore, the supernatant of PEA tissue was taken and checked via flow cytometry for inflammatory markers. In comparison to the factors measured, IL-8, MCP-1 and IL-6 were highly present (Fig.24). Besides their presence in the supernatant, they could be located with the help of IHC at tissue level in PEA material (Fig.25A-C). IL-8 and IL-6 seem to be located mainly in the cells forming vessels (ECs), whereas MCP-1 could be located in fibrocytes. IL-8 is known to be a ligand for the CXCR2 receptor, which is mediating angiogenesis, EC migration and endothelial recovery (63,64). MCP-1 is increased due to a response to injury caused by pressure overload or shear stress in CTEPH patients. Monocytes and macrophages get activated by the increased MCP-1 levels and therefore induce EC or SMC proliferation and matrix protein synthesis (65). IL-6 was shown in HUVECs to increase the adhesiveness for blood lymphocytes (66) and was suggested to be responsible for systemic vasoplegia in CTEPH patients after PEA treatment (67). Langer et al also observed a significant correlation between IL-6 level in serum and severity of the disease (67). Additionally IL-6 was suggested as a predictor for patients with increased risk for infection after PEA (68).

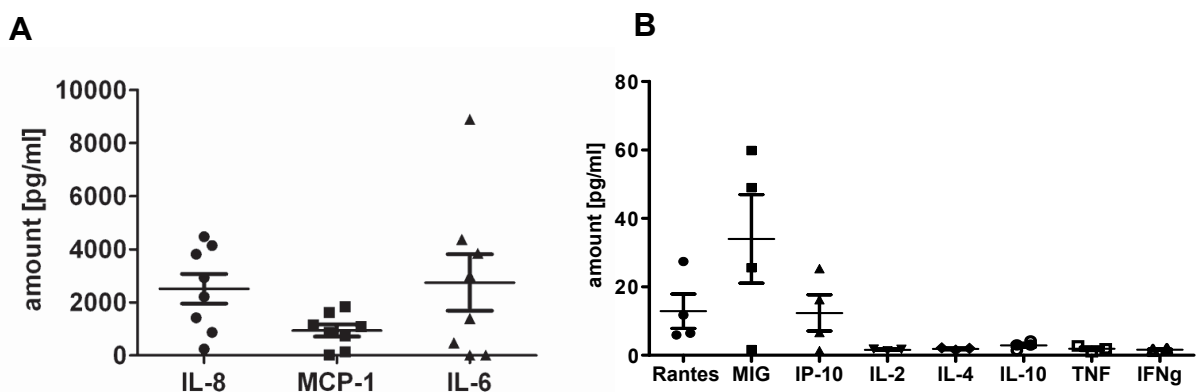


**Fig.24: Presence of IL-8, MCP-1 and IL-6 in the supernatant of PEA tissue.**

(A, B) Summarized results of flow cytometry measurements in the supernatant of PEA tissue obtained from 8 different patients. Amount of IL-8 ( $2514 \pm 558,1$  pg/ml), MCP-1 ( $937,7 \pm 227,9$  pg/ml) and IL-6 ( $2749 \pm 1065$  pg/ml). (B) Other factors are present in a less amount in PEA tissue.

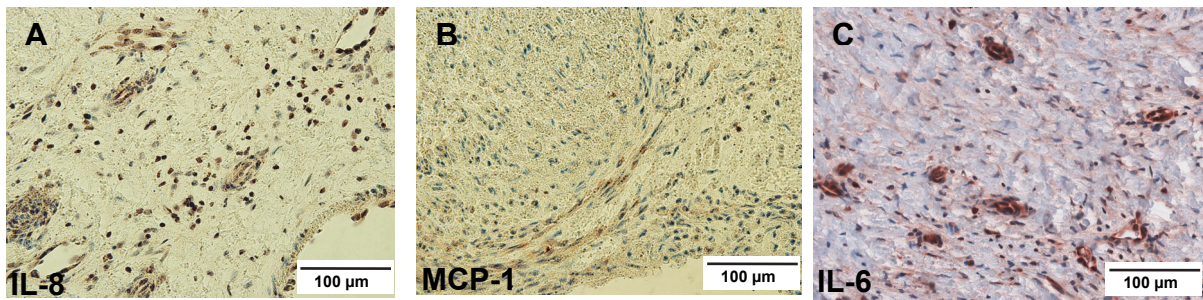


**Fig.25: Presence of IL-8, MCP-1 and IL-6 in PEA tissue.**

*PEA tissue staining for IL-8 (A), MCP-1 (B) and IL-6 (C).*

To confirm the presence of the inflammatory factors, we performed RT-PCR and checked the expression levels for IL-8, IL-6, MCP-1, IP-10, MIG and Rantes in the PEA tissue and compared them with human donor lung tissues (Fig.26). IL-8 showed no significance but a tendency in up-regulation. All other factors were significantly up-regulated in PEA tissue, whereas MIG in contrary showed a significant down-regulation compared to control lungs.

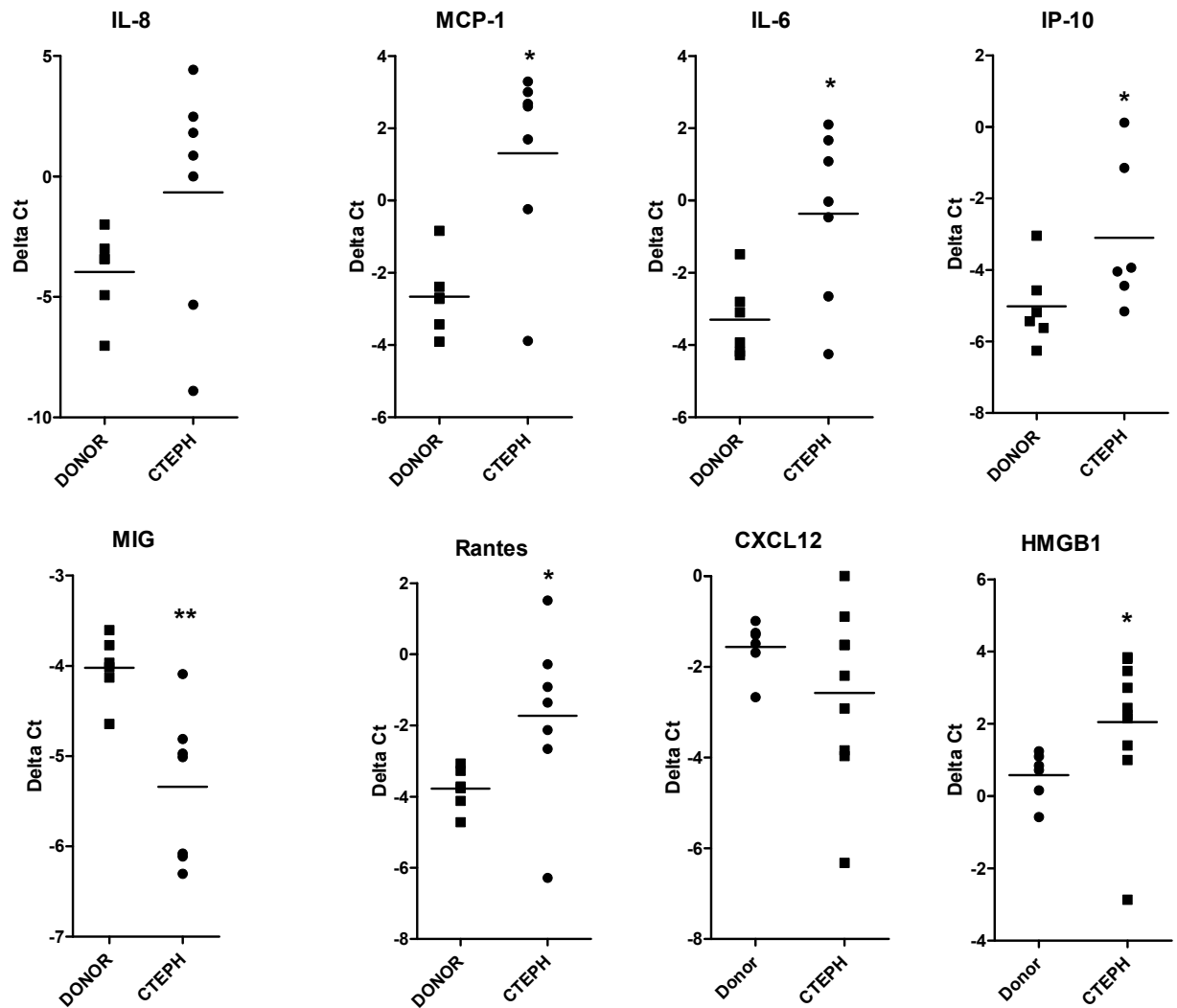


**Fig.26: Expression of inflammatory factors in PEA tissue compared to healthy human donor lungs.**

Relative expression of IL-8, MCP-1, IL-6, IP-10, MIG, Rantes, CXCL12 and HMGB1 in PEA tissue compared to human lungs (\*  $p < 0,05$ ; \*\*  $p < 0,01$  compared to control; Mann-Whitney test).

To observe the effect of the IL-8, MCP-1 and IL-6 cocktail on the hPAEC calcium homeostasis, the cells were incubated for 48h with the stimuli and than calcium changes due to histamine or BHQ challenge were measured (Fig.27). Only in case of store depletion an increased  $Ca^{2+}$  level after BHQ application could be observed in the hPAECs treated with the cocktail ( $p$ -value $<0,0001$ ) (Fig.27B). The basal calcium level as well as the calcium influx was not altered by the IL-8, IL-6 and MCP-1 cocktail treatment (Fig.27A, C).

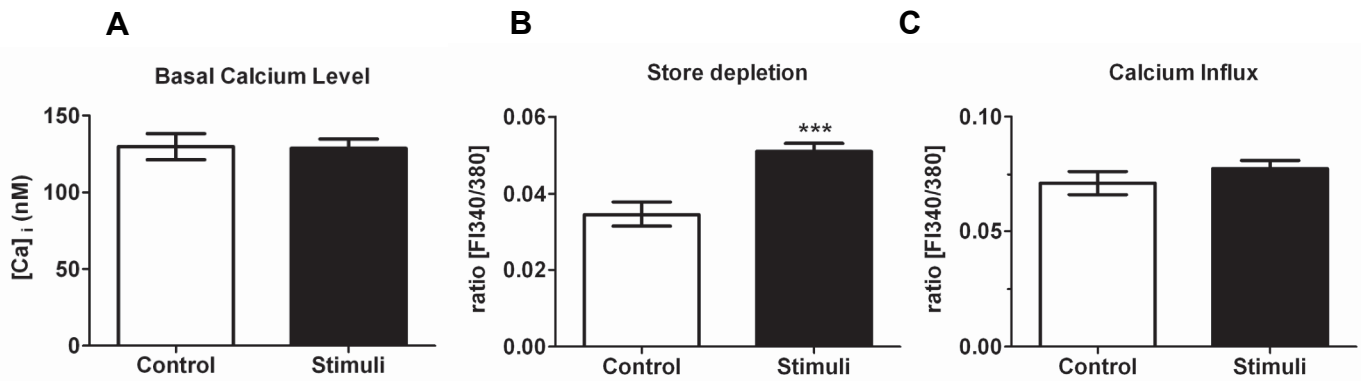


**Fig.27: Effect of IL-8, MCP-1 and IL-6 on hPAEC calcium homeostasis.**

(A) Basal calcium level of IL-8, MCP-1 and IL-6 cocktail stimulated hPAECs ( $0,051 \pm 0,002$  ratio [F1340/F1380];  $n=66$ ) compared to control hPAECs ( $0,035 \pm 0,003$  [F1340/F1380];  $n=45$ ). Store depletion (B) and calcium influx (C) of hPAECs stimulated with the cocktail ( $n=69$ ) compared to control cells ( $n=45$ ); (\*\*\*) =  $p < 0,001$  compared to control).

The process of thrombus formation is very complex and still not totally understood. An animal model for chronic total occlusion showed that the clot development can be divided in several steps, where after invasion of inflammatory cells vessel formation occurs (57-59). This step could be initiated by IL-8, which we found in the PEA tissue. It is reported in the literature to act angiogenic and therefore promotes vessel formation, which is needed for recanalization of the occluded regions (63,64,69).

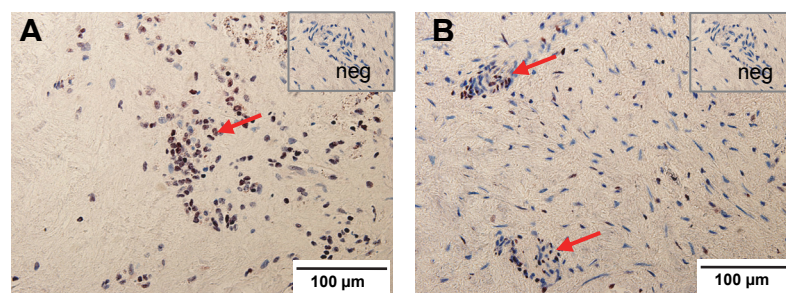


**Fig.28: Presence of IL-8 receptor CXCR2.**

(A and B) CXCR2 staining on PEA tissue. Dapi in blue represents the nuclei staining. Negative control shown as inset.

To initialize the angiogenesis process its receptor CXCR2 is needed. To confirm its presence in the PEA tissue immunohistochemical staining as well as RT-PCR were performed and indeed the receptor was detectable at protein and mRNA level (Fig.28, 29). Having a closer look at the CXCR2 expression level from PEA tissue compared to the healthy human lung it can be stated, that CXCR2 is 0,8 fold up-regulated in total PEA tissue (Fig.29). By dividing the PEA tissue into its localisation (distal or central), CXCR2 is 1,3 fold up-regulated in the central tissue piece, whereas it is only 0,4fold up-regulated in the distal PEA tissue compared to human lung tissue. This indicates that the PEA tissue shows a different expression pattern, dependent on its central or distal localisation.

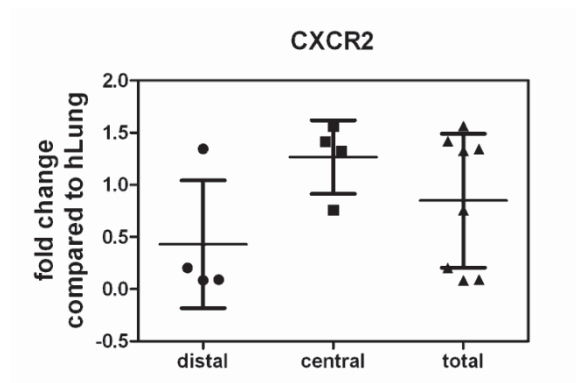


**Fig.29: RT-PCR expression of CXCR2 in PEA tissue and human lung.** Relative expression of CXCR2 in distal, central respectively total PEA tissue compared to human lung.

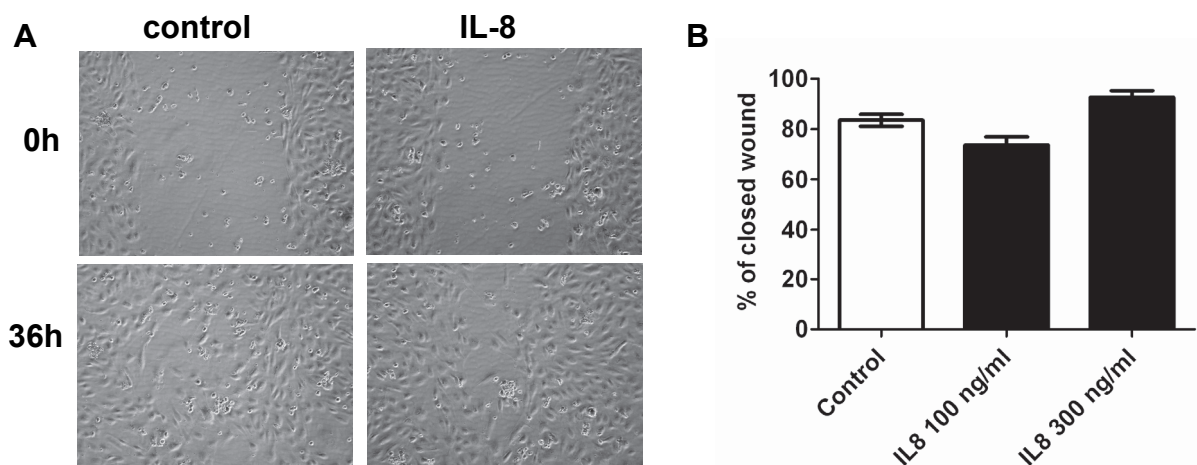


**Fig.30: Effect of IL-8 on hPAEC wound healing.**

(A) Representative images of migration assay showing the effect of IL-8 (100ng/ml) on hPAECs.  
 (B) Summarized results of wound healing after 36h IL-8 treatment ( $n_{exp}=3$ ).

Looking at the effect of IL-8 on the hPAEC migration (Fig.30A, B) no significant increase in wound closure could be observed, whereas a trend was detected with increased IL-8 (300ng/ml) concentration (Fig.30B). In case of proliferation hPAEC treated with 100ng/ml IL-8 ( $170 \pm 16$  %) showed a significant increase in proliferation compared to control cells (Fig.31). Looking at the chemotactic effect of IL-8 100ng/ml showed no effect ( $106 \pm 10$  %), whereas 400ng/ml treatment with IL-8 showed a non-significant increased ( $200 \pm 57$  %) in chemotaxis of hPAECs compared to control ( $100 \pm 7$  %) (Fig.32).

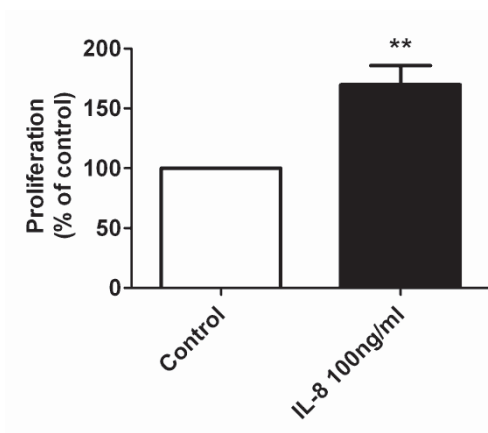


**Fig.31: Effect of IL-8 on hPAEC proliferation.**

Bar graph summarizing the effect of 100ng/ml IL-8 on hPAECs proliferation (\*\* =  $p < 0,01$ ). Readout was [ $^3$ H] thymidine incorporation.

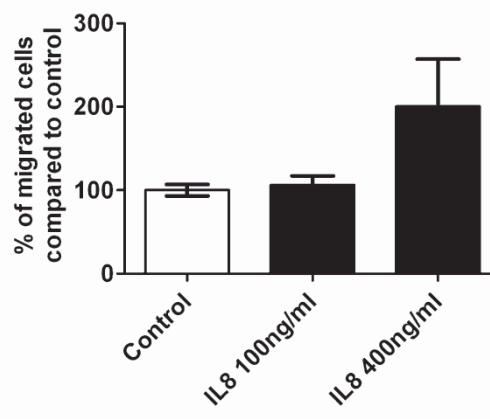


**Fig.32: Effect of IL-8 on hPAEC migration.**

The bars % of cells compared to control, which migrated to the bottom of the filter within 5h.

To sum up, we can state, that IL-8, MCP-1 and IL-6 are present in the supernatant of PEA tissue from CTEPH patients. We could validate these results with IHC stainings, showing their presence at tissue level as well as with the help of RT-PCR, where IL-8, MCP-1 and IL-6 was up-regulated in PEA tissue compared to healthy human lung tissue. Interestingly IP-10 as well as RANTES was up-regulated, whereas MIG showed a significant down-regulation in PEA tissue compared to control lungs. Challenging hPAECs with a cocktail of IL-8, MCP-1 and IL-6 we observed an increased depletion of the calcium stores. To observe how this calcium response could affect hPAECs we applied IL-8 on the cells and could observe an increased proliferation and migration in those cells, whereas there was no change in the wound healing.

## **PART 5**

---

### **Level of inflammatory factors in CTEPH serum**

To further investigate the inflammatory profile of the CTEPH patients and confirm the already presented data from the PEA supernatant, serum samples were taken and compared to age and sex matched healthy donors (Table 7).

**Table 7: Patient parameters**

	<b>CTEPH (n= 16)</b>	<b>Control (n= 16)</b>
<b>Age (years)</b>	62,56 [34-86]	62,18 [34-86]
<b>Gender (female, %)</b>	50	50
<b>mPAP preoperative (mmHg)</b>	45,88 ± 13,70	
<b>PVR preoperative (dyn·sec·cm<sup>-5</sup>)</b>	773,38 ± 329,31	
<b>CO preoperative (L·min<sup>-1</sup>)</b>	4,20 ± 1,15	
<b>CI preoperative (L·min<sup>-1</sup>·m<sup>-2</sup>)</b>	2,21 ± 0,51	

The inflammatory profile of the patients shows, that IL-8, IP-10, MIG, MIP1 $\alpha$ , IL-6 and HMGB1 are significantly increased in the serum of CTEPH patients compared to the serum of the donors. Interestingly RANTES is significantly decreased in the patients, whereas the presence of MCP-1 and CXCL12 is not significantly altered in CTEPH patients. (Fig.33, Table 8). This result is in line with the factors measured in the supernatant of PEA tissue (Fig.24) and the RT-PCR results of the PEA tissue (Fig.26). In both cases we could observe either the presence of IL-8, IL-6, MIP1 $\alpha$ , IP-10, MCP-1 and HMGB1 in the supernatant of PEA tissue or an up-regulation of those factors at mRNA level in PEA tissue compared to human lung tissue.

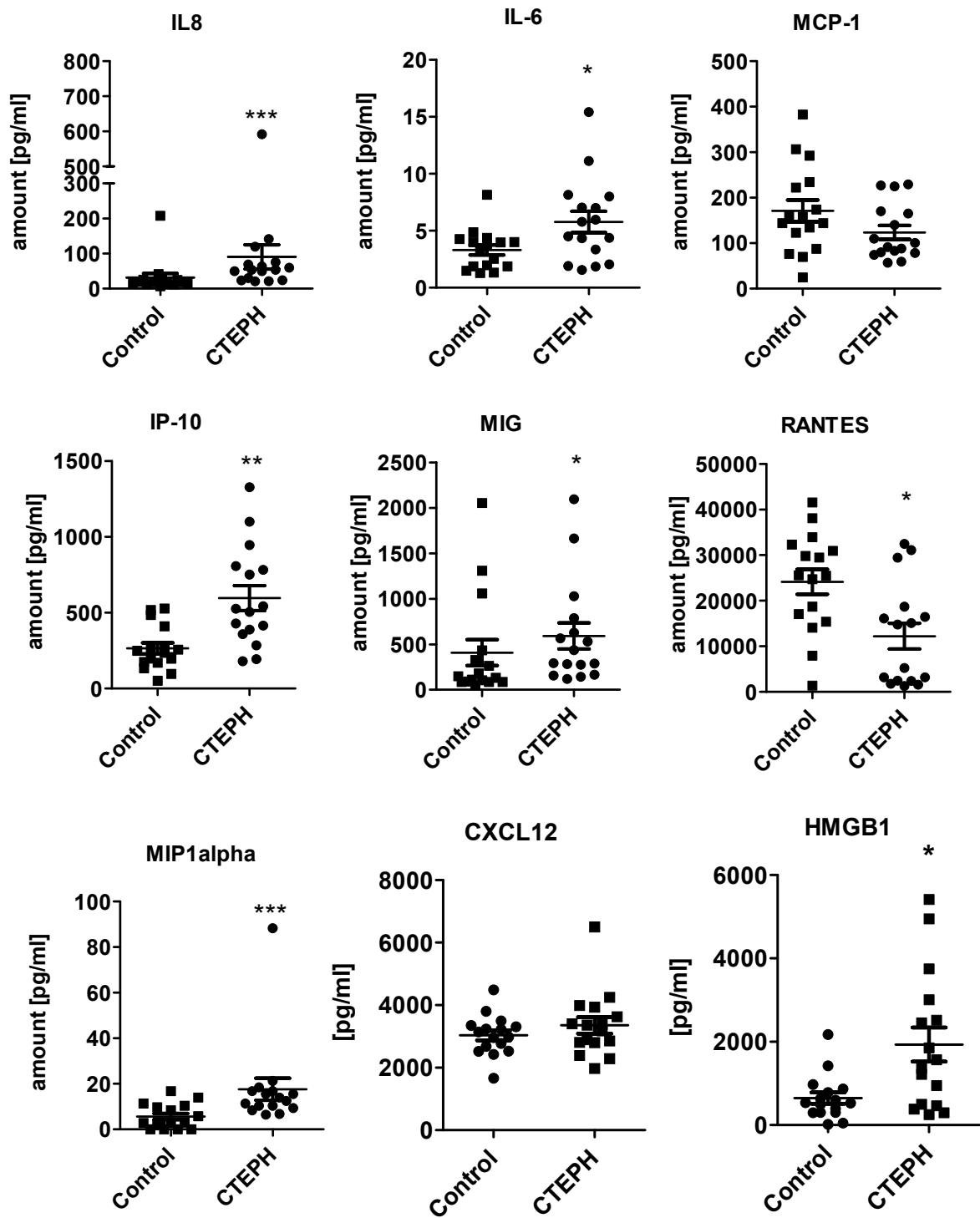


**Fig. 33: Presence of factors in serum of CTEPH-patients.**

Post PEA serum samples of CTEPH patients measured for inflammatory markers. Mann-Whitney test. \* $p < 0,05$ ; \*\* $p < 0,01$ ; \*\*\* $p < 0,001$

**Table 8: Summary of inflammatory factors measured in serum of CTEPH patients and Donors (\*p<0,05; \*\*p<0,01; \*\*\*p<0,001; mean ± SD)**

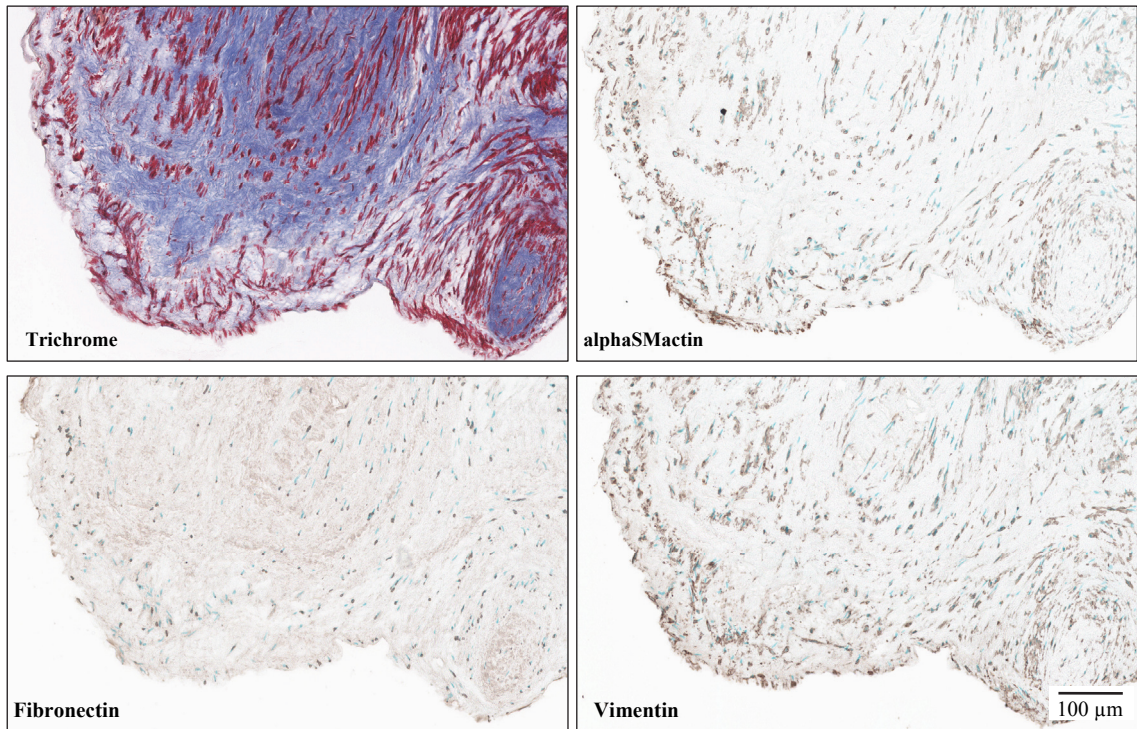
[pg/ml]	Control n=16	CTEPH n=16
<b>IL-8</b>	31,51 ± 47,68	90,51 ± 137,86 ***
<b>RANTES</b>	24155,9 ± 10993,19	12199,40 ± 11252,19 *
<b>MIG</b>	407,63 ± 570,72	591,36 ± 567,97 *
<b>MCP-1</b>	170,92 ± 95,75	123,71 ± 61,03
<b>IP-10</b>	265,11 ± 146,18	596,89 ± 328,83 **
<b>IL-6</b>	3,25 ± 1,82	7,07 ± 3,46 *
<b>MIP1alpha</b>	5,62 ± 5,42	17,62 ± 19,32 ***
<b>CXCL12</b>	3038,46 ± 640,58	2253,64 ± 1051,55
<b>HMGB1</b>	648,08 ± 537,32	1932,98 ± 1639,94

### **Fibroblast are present in the PEA tissue**

Another aspect of the stabilization of the clot is the role of fibroblasts in this process. The PEA tissue is rich in vimentin and fibronectin positive fibroblasts (Fig.34) and contains high amount of fibrotic material (Fig.4A, 5A), which accumulates over the years. The previously investigated factors (IL-8, IL-6, MCP-1, IP-10, MIP1alpha and HMGB1) found elevated in the serum of CTEPH patients and at RT-PCR level of PEA tissue could influence the migratory function of these fibroblasts, explaining their accumulation in the fibrotic clot, leading to further clot stabilization.

As a next step we investigated the expression profile of adventitial fibroblasts to check for their receptors. We could observe that fibroblasts from four different donors express CCR1, CCR5, IL6R, CXCR3, CXCR4, TLR4 and RAGE (Fig.35). This indicates that the receptor for MIP1alpha, RANTES, IL6, IP10, CXCL12 and HMGB1 are present and therefore those factors could have chemotactic effects on the cells, which leads to accumulation of fibroblasts in the thrombotic clot.

A



B

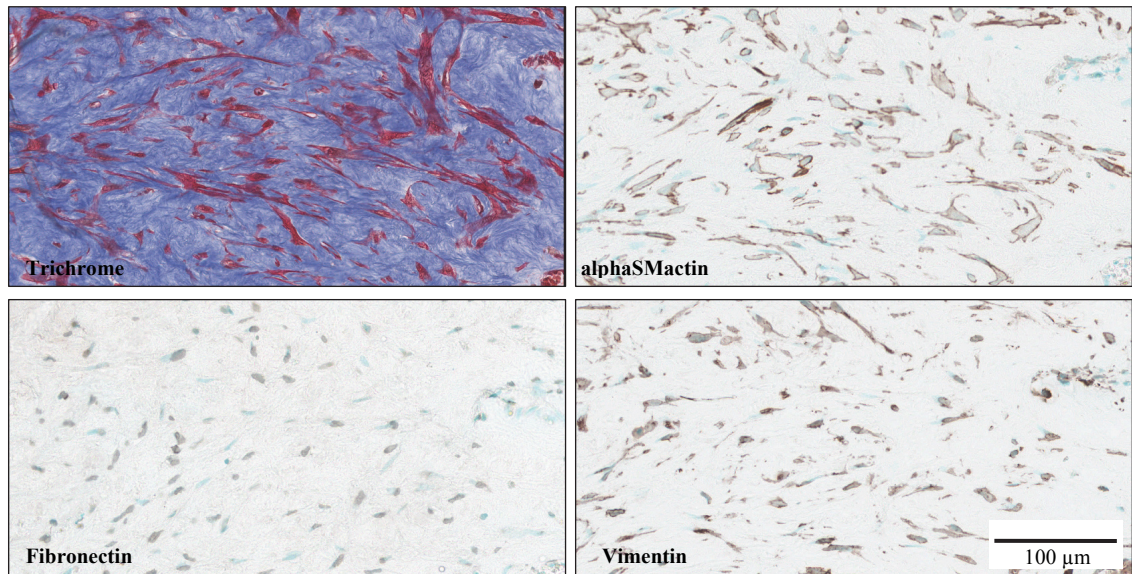


**Fig. 34: Presence of fibroblasts in PEA tissue**

A) Immunocytochemical staining for fibroblast markers B) Zoom in region

### Adv.Fibroblasts

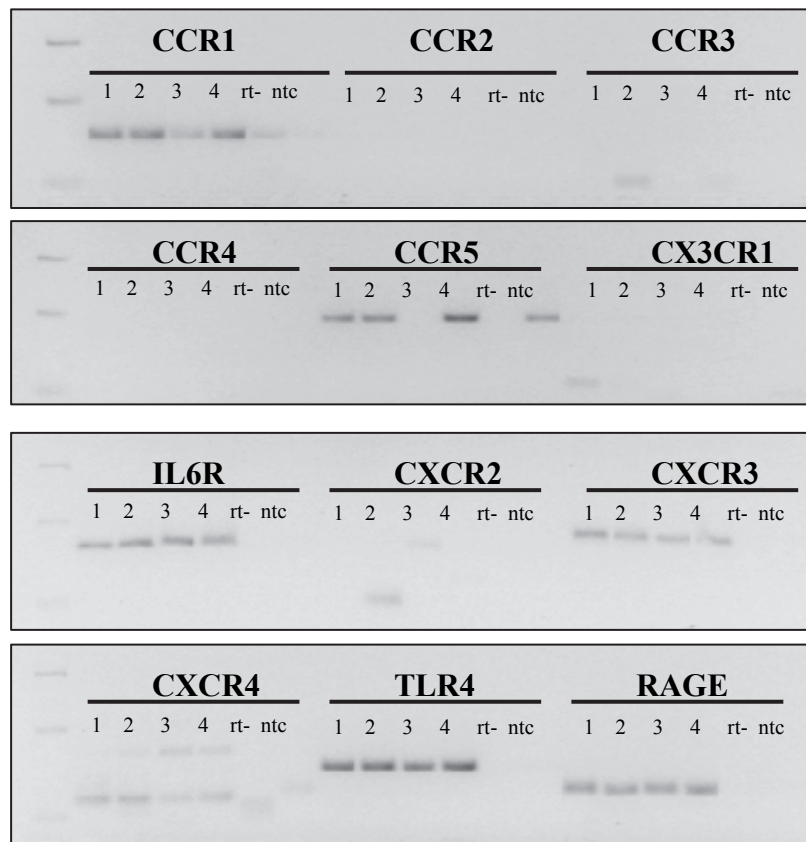
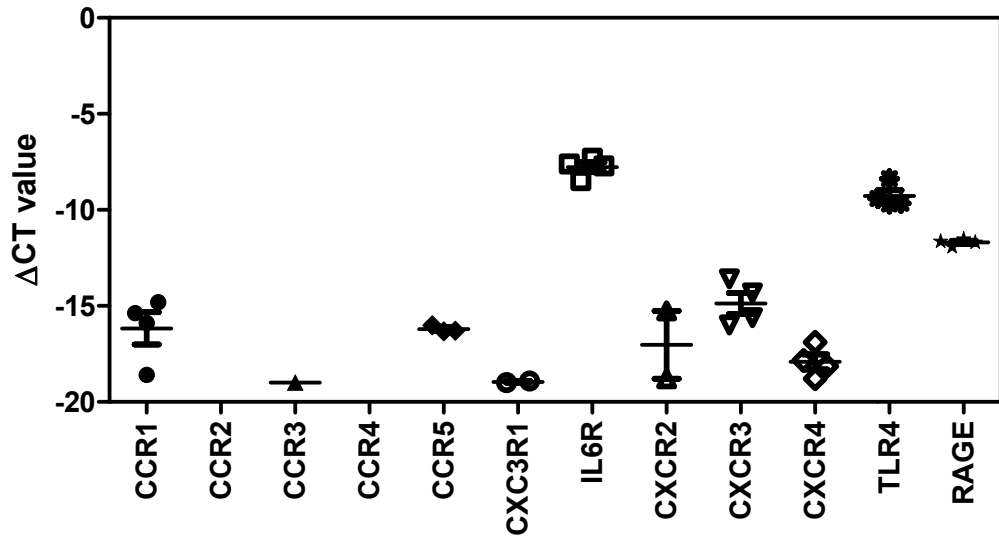


**Fig. 35: Receptor profile of Fibroblasts**  
 Performed in four different hPAEC donors (A) RT-PCR, (B) representative gel.

## Discussion

Chronic thromboembolic pulmonary hypertension (CTEPH) is a rare and late complication of venous thromboembolism. A fresh pulmonary embolus normally gets dissolved by macrophages (57,70,71) and by recanalization (58,59). In CTEPH patients, the recanalization does not occur or it is incomplete (6,17,72). In addition, a progressive occlusion occurs gradually resulting in elevation of pulmonary vascular resistance and secondary remodelling of non-occluded vessels.

In our study, we investigated endothelial cells from surgical PEA material (CTEPH-hECs), compared them with control hPAECs and tested the effect of circulating mediators and mediators secreted by the PEA material on hPAECs. Our readouts included calcium homeostasis, proliferation, migration and vessel formation. Similar to other groups (6,17,73), we observed newly formed vessels in the surgical PEA material. This neovascularization / recanalization has been suggested to be due to endothelial progenitor cells and/or hPAECs and pulmonary artery smooth muscle cells (PASMCs) migrating from the pulmonary artery or from the systemic circulation and being trapped in the thrombotic clot (15,17,23).

Endothelial cells from the blood-vessel wall interface control the coagulation processes, by expressing factors such as thrombomodulin, heparin-like molecules, vWF, protein S and tissue factor pathway inhibitor (74,75). To have an intact endothelial cell monolayer in the vessel after a lesion or injury, endothelial regeneration is essential. For the regeneration of the endothelial layer after a wound, migration and proliferation of endothelial cells is necessary (76). A key regulatory molecule for endothelial function is calcium (77). It was shown by several groups, that a range of inflammatory stimuli can increase the intracellular calcium concentrations and activate downstream pathways, leading for example to increased microvascular permeability or vascular leakage pointing to endothelial dysfunction (78,79). On the other side, increase in intracellular calcium also lead to the up-regulation of transcription factors needed for the initialization of cell motility

after damaging of the endothelial layer (80). An elevated intracellular calcium level increases NO production, promoting endothelial cell proliferation (81).

The reason why in CTEPH patients a persistent occlusion is present in the pulmonary arteries is still not well known. It is suggested that endothelial dysfunction may play a role, leading to a deregulation of the thrombus resolution process, altered signalling for initializing proliferation, migration and/or permeability. To elucidate possible dysfunction in the endothelial cells received from the PEA material (CTEPH-hECs) we investigated the calcium homeostasis of these cells upon histamine or BHQ stimulation and compared their intracellular calcium levels to healthy hPAECs. Histamine acts over G-protein coupled receptor leading to an increase in intracellular calcium, whereas BHQ an ATPase blocker of the sarcoendoplasmic reticulum leads to calcium store depletion and secondary to increased calcium influx over the store operated calcium channels present on the plasma membrane. We observed a significant rise in the basal calcium level of the CTEPH-hECs as compared to the hPAECs. Furthermore, in our study histamine challenge led to a stronger response in the CTEPH-hECs as compared to hPAECs. We applied a calcium ATPase inhibitor (BHQ) to induce depletion of the calcium stores (37) and to identify the reason for this calcium rise. By readmission of the external calcium, the store-operated calcium influx was quantified and compared to healthy control cells. With this tool, possible dysfunctions either in calcium channels of the plasma membrane or in the calcium stores can be detected (37). The increased calcium depletion of the CTEPH-hECs compared to hPAECs showed that these cells accumulate more calcium in their stores, which is a sign of altered calcium homeostasis (82). In our study, the influx of external calcium was greater in the CTEPH-hECs compared to control cells. One possible reason for this increase could be the higher expression or sensitivity of TRPC channels in the plasma membrane, as previously described in PSMCs isolated from patients with idiopathic pulmonary arterial hypertension (IPAH) (83). The increased intracellular calcium level observed in CTEPH-hECs could also be a hint for initialization of downstream signalling pathways leading to altered endothelial cell behaviour such as altered proliferation or migration. Indeed the CTEPH-hECs showed an increased proliferation compared to hPAECs. Beside the altered calcium homeostasis and proliferation, the CTEPH-hECs showed a typical endothelial phenotype: cobblestone monolayer formation, expression of vWF and

continuous VE-cadherin membrane staining. No significant differences in vessel formation and wound closure properties were observed in CTEPH-hECs compared to the hPAECs.

Sakao et al. have recently reported that isolated EC-like cells from surgical PEA material exhibit a defective mitochondrial structure, inability to form autophagosomes and morphologic changes after some passages (72). They suggest that the microenvironment present in the PEA material may cause endothelial dysfunction as observed in their study (72). Another study suggested that this microenvironment caused hyperproliferation, invasiveness, and anchorage independent growth of myofibroblasts (84). Therefore we elucidated possible factors from the microenvironment of the thrombotic clot, which could lead to altered endothelial behaviour. In our study, we identified three factors which may cause endothelial dysfunction. The expression of PF4, collagen type I and IP-10 were visualized in the surgical PEA material. All these proteins were quantified in the supernatant of the tissue. PF4 (also known as CXCL4) is exclusively expressed in developing megakaryocytes and stored in  $\alpha$ -granules of platelets. Activated platelets release PF4 at sites of injury (85,86). IP-10 (also known as CXCL10) is reported to activate and recruit effector T cells and other leukocytes (87) and is strongly up-regulated in many inflammatory diseases (88). Finally, collagen type I is important for wound healing and formation of extracellular matrix, which may promote proliferation of  $SM\alpha Actin^+$  cells and differentiation of injured ECs into  $SM\alpha Actin^+$  cells (17). Based on these previous results, these factors may harbour angiostatic features in the PEA material potentially contributing to the development of CTEPH.

To elucidate the effects of the factors which we found in the microenvironment of the PEA material we challenged hPAECs with PF4, collagen type I and IP-10 and checked for alterations in calcium handling of those cells. Only collagen and 24h IP-10 increased the basal calcium level, while store depletion and calcium influx were increased by collagen type I, as well as by IP-10 and PF4. Only fibrin and thrombin have been shown previously to increase basal calcium levels in EC from PEA material (18). This suggests that the microenvironment of the surgical PEA material significantly affects the calcium homeostasis of the endothelial cells. The

question, how PF4 and IP-10 may evoke angiostatic effects in hPAECs is still unsolved. PF4 and IP-10 are known to be ligands for CXCR3 (89,90). Romagnani et al. showed that human microvascular endothelial cells express CXCR3 which mediates angiostatic effects (90). In their study the percentage of CXCR3 positive vessels in diseased tissue was significantly higher compared to healthy tissue. We detected CXCR3 expression in hPAECs as well as in CTEPH-hECs, indicating that its ligands, IP10 and PF4, might evoke an angiostatic effect by activating CXCR3. PEA material, compared to human lung, showed abundant CXCR3, visualised by immunohistochemistry particularly in the vessels. On the mRNA level, CXCR3 was up-regulated in the distal PEA areas as compared to control lung. In addition, a hallmark for chemokine activation is the ability to initiate calcium signalling (91), mainly via G-protein coupled receptors. It has been reported previously that stimulation of CXCR3 leads to mobilization of intracellular calcium (91-94). Thus, our results suggest that PF4 and IP-10 via CXCR3 activation might lead to endothelial dysfunction and altered angiogenesis.

Vessel formation and migration are important features of ECs (95). PF4 is thought to act as an angiostatic factor by interacting with pro-angiogenic molecules such as VEGF or FGF, cell adhesion molecules and integrins (96-98). In addition, PF4 has been shown by Yang et al to inhibit the migration of human endothelial progenitor cells, as well as suppressing microvessel formation in myeloma xenografts (60). In our study we also observed the angiostatic effect of PF4. By treating hPAECs with PF4 significantly decreased their migration and vessel formation. Furthermore, we observed an inhibition of hPAEC proliferation by PF4 treatment, supporting the angiostatic effect of PF4.

Additionally to PF4, we also showed, that collagen type I is present in the microenvironment of the PEA tissue. As already mentioned, collagen type I has an effect on the calcium homeostasis of hPAECs. Due to the increased intracellular calcium level, downstream signalling pathways could be activated. It was shown by Paria et al that cells treated with TNFalpha lead to a two-fold increase in thrombin-induced calcium influx in hPAECs (99). This calcium influx was shown to be dependent on TRPC1 signalling, because they observed that TNFalpha stimulation in hPAECs led to an increased expression of TRPC1. By over

expressing TRPC1 in human microvascular endothelial cells (HMVECs), the thrombin-induced calcium influx also showed a two-fold increase (99). In our study we could also observe an increased intracellular calcium level upon collagen type I treatment. Paria et al showed a nice connection between TRPC1 up-regulation upon TNF $\alpha$  treatment leading to increased calcium influx and resulting in accumulation of actin-stress fibre formation and increased endothelial permeability. Similar results were shown by Ye et al 2005, who observed that in acute lung injury Pre-B-cell-colony-enhancing factor (PBEF) is up-regulated, leading to increased intracellular calcium and permeability (100). In our study we could observe upon collagen type I treatment an increased permeability in hPAECs. It could be that the collagen type I induced permeability is also TRPC1 driven, but this has to be investigated in more detail. We could show that this increase in permeability was due to decrease cell-cell contacts, which was shown by a decrease in VE-cadherin signal after collagen type I treatment. Beside permeability also proliferation and migration was altered. This could also explain the observed decrease in vessel formation after collagen application.

Finally, IP-10 was also elevated in PEA material in our study. Angiolillo et al. showed that IP-10 did not inhibit HUVEC proliferation, but suppressed HUVEC differentiation into capillary structures (61,101). However, in HUVECs, HMVECs and cardiac ECs, IP-10 had anti-proliferative effects (88). Additionally IP-10 has been reported to act as an angiostatic factor *in vivo* (102) and *in vitro* (62). This is in line with our observations, where we observed a significant decrease in vessel formation in hPAECs upon IP-10 treatment. In contrary we could not observe changes in migration, permeability nor decrease in proliferation.

Our data indicate that PF4, collagen type I and IP-10 interfere with endothelial vessel-forming ability *in vitro*, explaining the decreased vessel formation in PEA tissue and therefore the inhibited recanalization process. This might lead to a stabilization of the thrombus in CTEPH patients resulting in a pulmonary pressure increase.

CTEPH develops due to progressive pulmonary vascular occlusion. Firth et al observed an accumulation of fibroblasts and myofibroblasts in the PEA tissue (14). In addition to these findings, we detected collagen depositions and the presence of

endothelial and smooth muscle cells, which participate in the partial recanalization of the clot. In the first step of thrombus resolution inflammatory cells get attracted to invade the clot, as it was shown by Jaffe et al in a rabbit chronic total occlusion model (25). But how the process gets misguided? A recent review (103) suggests that in the early phase of wound healing cytokines, which stimulate extracellular matrix (ECM) synthesis, are produced and later on they are repressed once wound healing is completed. Additionally apoptotic gene programs are activated in myofibroblasts (104) terminating the ECM synthesis and progressive proliferation. Interestingly in fibrosis, failure of initiating myofibroblast apoptosis was observed. Therefore they stay persistent and continue the ECM formation (103). This would explain the presence of collagen in the PEA tissue, which we detected in the supernatant of PEA tissue and via trichrome staining. We also observed the presence of fibroblast with the help of vimentin, fibronectin and alpha smooth muscle staining in PEA tissue. To elucidate which factors could attract fibroblasts into the fibrotic clot, where they continue the ECM formation, we measured in the supernatant of PEA tissue and in the serum of CTEPH patients inflammatory factors such as RANTES, MIG, IP-10, IL-2, IL-4; IL-10, TNF, IF $\gamma$ , IL-8, MCP-1 and IL-6 and investigated their expression at mRNA level in PEA tissue. We observed the presence of IL-8, IL-6 and MCP-1 in the supernatant of the PEA tissue as well as an up-regulation of those factors at mRNA level compared to donor lung tissue.

MCP-1 was shown by Brian L Hoh to promote migration of macrophages, fibroblast, smooth muscle cells and endothelial cells to the place of injury (105). It plays an important role in inflammatory healing in extravascular tissue (cutaneous wound and myocardial infarction). In the intravascular environment MCP-1-induced inflammation can lead to neointimal hyperplasia (106-110), atherosclerosis and increased proliferation (111). The four cell types attracted by MCP-1 play different roles in wound healing. Macrophages initiate inflammatory healing, fibroblasts lead to connective tissue proliferation, endothelial cells are important for capillary in growth and smooth muscle cells for vascular integrity (105). In a model of myocardial infarction it was shown, that MCP-1 is important for macrophage infiltration, neovascularisation and accumulation of cardiac myofibroblasts (112). The elevated level of MCP-1 in the supernatant of PEA tissue found in our study could be a hint for attraction of myofibroblast and

macrophages into the PEA tissue of CTEPH patients. In addition, MCP-1 also stimulates fibroblast proliferation and collagen secretion (113) which may lead to persistent occlusion of the vessel. Furthermore MCP-1 might serve as a biomarker, since MCP-1 is up-regulated in plasma of CTEPH patients in response to increased vascular resistance (65). The same up-regulation was observed in our patient cohort.

Besides MCP-1, IL-8 was detected in the supernatant of PEA tissue and we observed that its mRNA expression was increased in PEA tissue compared to donor lung. We assume, that IL-8 initiates invasion of inflammatory and vascular cells into occluded area. IL-8 is acting over its receptor CXCR2 (114). To confirm its presence in the PEA tissue immunohistochemical staining as well as RT-PCR were performed. The receptor was detectable at protein and mRNA level. The presence of IL-8 receptor was shown in HUVECs by Koch et al (114). His group also showed that IL-8 increased proliferation and chemotaxis in HUVECs. In our study we could show that IL-8 increased chemotaxis and proliferation in hPAECs, whereas the wound healing was not altered. For chemotaxis cytoskeletal response is necessary, therefore Schraufstatter et al looked at the effect of IL-8 on filamentous actin (F-actin) filament formation in cultured endothelial cells. They observed, that IL-8 caused cytoskeletal rearrangement due to activation of both the CXCR1 and the CXCR2 (115). This could be also the reason for the increased chemotaxis we observed in hPAECs upon IL-8 stimulation. Li et al also observed increased endothelial cell proliferation, migration and capillary tube organization upon IL-8 stimulation (69). The endothelial cells showed after IL-8 stimulation inhibition in cell apoptosis and enhanced antiapoptotic gene expression. Furthermore matrix metalloproteinase (MMP) expression and production was elevated due to IL-8 stimulation, which would facilitate migration of endothelial cells due to degradation of extracellular matrix (69,116). This might indicate that the observed proliferation and migration in hPAECs by us are due to decreased apoptosis and that the IL-8 induced MMP expression and production could facilitate the cellular invasion into the PEA tissue.

Soon et al recently showed an increased level of inflammatory cytokines (IL-1b, IL-2, IL-4, IL-8 and IL-10) in CTEPH patients compared to healthy controls (117).

They defined IL-6 and IL-8 as useful biomarkers to identify patients at risk developing residual pulmonary hypertension after PEA surgery. In our study we investigated the presence of RANTES, MIG, IP-10, IL-8, MCP-1, IL-6 and MIP1alpha in the serum of CTEPH patients and compared them with healthy donors. We could detect, that IL-8, IL-6, IP-10 and MIP1alpha are significantly increased in the serum of CTEPH patients. The same factors were also up-regulated in PEA tissue compared to human lung.

An important factor in the PEA tissue and therefore also in CTEPH are the fibroblasts. As previously shown, the PEA tissue is highly fibrotic and contains fibroblasts. The question arises what factors could attract those cells into the fibrotic tissue. The factors we could identify as up-regulated in the tissue and highly present in the serum, namely IL-8, IL-6, IP-10 and MIP1alpha, could be interesting candidates as chemoattractants for those cells. A possibility to validate this hypothesis is by performing chemotaxis studies with these factors on fibroblasts.

In summary, we observed altered calcium homeostasis, manifested by elevated basal calcium level, increased store depletion and calcium influx in endothelial cells from surgical PEA material. In addition the presence of angiostatic factors as well as their receptor could be detected. Furthermore, our investigations show that angiostatic factors by partially increasing the basal calcium level as well as store depletion and calcium influx, alter the calcium handling in normal hPAECs, leading to the conclusion that the microenvironment in PEA material might contribute to the altered calcium homeostasis in CTEPH-hECs. These observations suggest that IP-10, collagen and PF4 lead to angiostatic effects, shown by decreased angiogenesis and/or proliferation and migration. As a consequence there might be inadequate recanalization of the thromboembolic material, which leads to persistent increase in pulmonary pressure.

In addition, we could observe the presence of inflammatory factors, such as MCP-1, IL-8 and IL-6 in the supernatant of PEA tissue and via IHC. Stimulating hPAECs with these three factors led to an increase in depletion of the calcium stores, which could lead to increased proliferation. Examining the effect of IL-8, we could observe increased proliferation and chemotaxis in hPAECs. This indicates that

factors initiating angiogenesis are present in the PEA material, but it seems that these factors are not strong enough to overcome the effect of the angiostatic factors. This could explain on the one hand the observations from the PEA material, where partial recanalization occurred, which could be due to the presence of MCP-1 and IL-8. On the other hand the presence of the angiostatic factors such as collagen, PF4 and IP-10 inhibit the already started angiogenic process. Another problem could be that during a lifespan of a CTEPH patient all the time small thrombi accumulate in the main thrombus, which could always reinitialize the resolution process of the thrombus, therefore an angiogenic/angiostatic unbalance could occur in CTEPH patients disturbing the resolution process of thrombi.

## References

- (1) Lang I. Advances in understanding the pathogenesis of chronic thromboembolic pulmonary hypertension. *Br J Haematol* 2010 Mar 16;149(4):478-483.
- (2) Mogi K, Nakajima N, Masuda M, Hayashida N, Pearce Y, Nakaya M. A study on the role of platelet function in patients with chronic pulmonary thromboembolism. *Ann Thorac Cardiovasc Surg* 2001 Jun;7(3):133-137.
- (3) Archer S, Rich S. Primary pulmonary hypertension: a vascular biology and translational research "Work in progress". *Circulation* 2000 Nov 28;102(22):2781-2791.
- (4) Auger WR, Fedullo PF. Chronic thromboembolic pulmonary hypertension. *Semin Respir Crit Care Med* 2009 Aug;30(4):471-483.
- (5) Miniati M, Monti S, Bottai M, Scoscia E, Bauleo C, Tonelli L, et al. Survival and restoration of pulmonary perfusion in a long-term follow-up of patients after acute pulmonary embolism. *Medicine (Baltimore)* 2006 Sep;85(5):253-262.
- (6) Moser KM, Bloor CM. Pulmonary vascular lesions occurring in patients with chronic major vessel thromboembolic pulmonary hypertension. *Chest* 1993 Mar;103(3):685-692.
- (7) Ryan KL, Fedullo PF, Davis GB, Vasquez TE, Moser KM. Perfusion scan findings understate the severity of angiographic and hemodynamic compromise in chronic thromboembolic pulmonary hypertension. *Chest* 1988 Jun;93(6):1180-1185.
- (8) Azarian R, Wartski M, Collignon MA, Parent F, Herve P, Sors H, et al. Lung perfusion scans and hemodynamics in acute and chronic pulmonary embolism. *J Nucl Med* 1997 Jun;38(6):980-983.
- (9) Bresser P, Pepke-Zaba J, Jais X, Humbert M, Hoepfer MM. Medical therapies for chronic thromboembolic pulmonary hypertension: an evolving treatment paradigm. *Proc Am Thorac Soc* 2006 Sep;3(7):594-600.
- (10) Ulrich S, Speich R, Domenighetti G, Geiser T, Aubert JD, Rochat T, et al. Bosentan therapy for chronic thromboembolic pulmonary hypertension. A national open label study assessing the effect of Bosentan on haemodynamics, exercise capacity, quality of life, safety and tolerability in patients with chronic thromboembolic pulmonary hypertension (BOCTEPH-Study). *Swiss Med Wkly* 2007 Oct 20;137(41-42):573-580.
- (11) Suntharalingam J, Treacy CM, Doughty NJ, Goldsmith K, Soon E, Toshner MR, et al. Long-term use of sildenafil in inoperable chronic thromboembolic pulmonary hypertension. *Chest* 2008 Aug;134(2):229-236.

- (12) Lang IM, Klepetko W. Chronic thromboembolic pulmonary hypertension: an updated review. *Curr Opin Cardiol* 2008 Nov;23(6):555-559.
- (13) Dartevelle P, Fadel E, Mussot S, Chapelier A, Herve P, de Perrot M, et al. Chronic thromboembolic pulmonary hypertension. *Eur Respir J* 2004 Apr;23(4):637-648.
- (14) Firth AL, Yao W, Ogawa A, Madani MM, Lin GY, Yuan JX. Multipotent mesenchymal progenitor cells are present in endarterectomized tissues from patients with chronic thromboembolic pulmonary hypertension. *Am J Physiol Cell Physiol* 2010 May;298(5):C1217-25.
- (15) Ogawa A, Firth AL, Yao W, Madani MM, Kerr KM, Auger WR, et al. Inhibition of mTOR attenuates store-operated Ca<sup>2+</sup> entry in cells from endarterectomized tissues of patients with chronic thromboembolic pulmonary hypertension. *Am J Physiol Lung Cell Mol Physiol* 2009 Oct;297(4):L666-76.
- (16) Golovina VA, Platoshyn O, Bailey CL, Wang J, Limsuwan A, Sweeney M, et al. Upregulated TRP and enhanced capacitative Ca<sup>2+</sup> entry in human pulmonary artery myocytes during proliferation. *Am J Physiol Heart Circ Physiol* 2001 Feb;280(2):H746-55.
- (17) Yao W, Firth AL, Sacks RS, Ogawa A, Auger WR, Fedullo PF, et al. Identification of putative endothelial progenitor cells (CD34+CD133+Flk-1+) in endarterectomized tissue of patients with chronic thromboembolic pulmonary hypertension. *Am J Physiol Lung Cell Mol Physiol* 2009 Jun;296(6):L870-8.
- (18) Firth AL, Yau J, White A, Chiles PG, Marsh JJ, Morris TA, et al. Chronic exposure to fibrin and fibrinogen differentially regulates intracellular Ca<sup>2+</sup> in human pulmonary arterial smooth muscle and endothelial cells. *Am J Physiol Lung Cell Mol Physiol* 2009 Jun;296(6):L979-86.
- (19) Morris TA, Marsh JJ, Chiles PG, Kim NH, Noskovack KJ, Magana MM, et al. Abnormally sialylated fibrinogen gamma-chains in a patient with chronic thromboembolic pulmonary hypertension. *Thromb Res* 2007;119(2):257-259.
- (20) Morris TA, Marsh JJ, Chiles PG, Auger WR, Fedullo PF, Woods VL, Jr. Fibrin derived from patients with chronic thromboembolic pulmonary hypertension is resistant to lysis. *Am J Respir Crit Care Med* 2006 Jun 1;173(11):1270-1275.
- (21) Suntharalingam J, Goldsmith K, van Marion V, Long L, Treacy CM, Dudbridge F, et al. Fibrinogen Aalpha Thr312Ala polymorphism is associated with chronic thromboembolic pulmonary hypertension. *Eur Respir J* 2008 Apr;31(4):736-741.
- (22) Sakamaki F, Kyotani S, Nagaya N, Sato N, Oya H, Nakanishi N. Increase in thrombomodulin concentrations after pulmonary thromboendarterectomy in chronic thromboembolic pulmonary hypertension. *Chest* 2003 Oct;124(4):1305-1311.

- (23) Sacks RS, Remillard CV, Agange N, Auger WR, Thistlethwaite PA, Yuan JX. Molecular biology of chronic thromboembolic pulmonary hypertension. *Semin Thorac Cardiovasc Surg* 2006 Fall;18(3):265-276.
- (24) Ellis CA, Tiruppathi C, Sandoval R, Niles WD, Malik AB. Time course of recovery of endothelial cell surface thrombin receptor (PAR-1) expression. *Am J Physiol* 1999 Jan;276(1 Pt 1):C38-45.
- (25) Jaffe R, Leung G, Munce NR, Thind AS, Leong-Poi H, Anderson KJ, et al. Natural history of experimental arterial chronic total occlusions. *J Am Coll Cardiol* 2009 Mar 31;53(13):1148-1158.
- (26) Mayer E, Klepetko W. Techniques and outcomes of pulmonary endarterectomy for chronic thromboembolic pulmonary hypertension. *Proc Am Thorac Soc* 2006 Sep;3(7):589-593.
- (27) Hoeper MM, Mayer E, Simonneau G, Rubin LJ. Chronic thromboembolic pulmonary hypertension. *Circulation* 2006 Apr 25;113(16):2011-2020.
- (28) Moser KM, Auger WR, Fedullo PF. Chronic major-vessel thromboembolic pulmonary hypertension. *Circulation* 1990 Jun;81(6):1735-1743.
- (29) Jamieson SW, Kapelanski DP, Sakakibara N, Manecke GR, Thistlethwaite PA, Kerr KM, et al. Pulmonary endarterectomy: experience and lessons learned in 1,500 cases. *Ann Thorac Surg* 2003 Nov;76(5):1457-62; discussion 1462-4.
- (30) Klepetko W, Mayer E, Sandoval J, Trulock EP, Vachieri JL, Darteville P, et al. Interventional and surgical modalities of treatment for pulmonary arterial hypertension. *J Am Coll Cardiol* 2004 Jun 16;43(12 Suppl S):73S-80S.
- (31) Rubin LJ, Hoeper MM, Klepetko W, Galie N, Lang IM, Simonneau G. Current and future management of chronic thromboembolic pulmonary hypertension: from diagnosis to treatment responses. *Proc Am Thorac Soc* 2006 Sep;3(7):601-607.
- (32) Darteville P, Fadel E, Chapelier A, Macchiarini P, Cerrina J, Parquin F, et al. Angioscopic video-assisted pulmonary endarterectomy for post-embolic pulmonary hypertension. *Eur J Cardiothorac Surg* 1999 Jul;16(1):38-43.
- (33) Thistlethwaite PA, Mo M, Madani MM, Deutsch R, Blanchard D, Kapelanski DP, et al. Operative classification of thromboembolic disease determines outcome after pulmonary endarterectomy. *J Thorac Cardiovasc Surg* 2002 Dec;124(6):1203-1211.
- (34) Fedullo PF, Auger WR, Kerr KM, Rubin LJ. Chronic thromboembolic pulmonary hypertension. *N Engl J Med* 2001 Nov 15;345(20):1465-1472.
- (35) Dietrich A, Kalwa H, Fuchs B, Grimminger F, Weissmann N, Gudermann T. In vivo TRPC functions in the cardiopulmonary vasculature. *Cell Calcium* 2007 Aug;42(2):233-244.

- (36) Ahmmed GU, Malik AB. Functional role of TRPC channels in the regulation of endothelial permeability. *Pflugers Arch* 2005 Oct;451(1):131-142.
- (37) Nilius B, Droogmans G. Ion channels and their functional role in vascular endothelium. *Physiol Rev* 2001 Oct;81(4):1415-1459.
- (38) Moncada S, Vane JR. Arachidonic acid metabolites and the interactions between platelets and blood-vessel walls. *N Engl J Med* 1979 May 17;300(20):1142-1147.
- (39) Moncada S, Palmer RM, Higgs EA. Nitric oxide: physiology, pathophysiology, and pharmacology. *Pharmacol Rev* 1991 Jun;43(2):109-142.
- (40) Loskutoff DJ, Edgington TE. Synthesis of a fibrinolytic activator and inhibitor by endothelial cells. *Proc Natl Acad Sci U S A* 1977 Sep;74(9):3903-3907.
- (41) Huber K, Beckmann R, Frank H, Kneussl M, Mlczoch J, Binder BR. Fibrinogen, t-PA, and PAI-1 plasma levels in patients with pulmonary hypertension. *Am J Respir Crit Care Med* 1994 Oct;150(4):929-933.
- (42) Eisenberg PR, Lucore C, Kaufman L, Sobel BE, Jaffe AS, Rich S. Fibrinopeptide A levels indicative of pulmonary vascular thrombosis in patients with primary pulmonary hypertension. *Circulation* 1990 Sep;82(3):841-847.
- (43) Ryan US, Avdonin PV, Posin EY, Popov EG, Danilov SM, Tkachuk VA. Influence of vasoactive agents on cytoplasmic free calcium in vascular endothelial cells. *J Appl Physiol* 1988 Nov;65(5):2221-2227.
- (44) Berridge MJ. Capacitative calcium entry. *Biochem J* 1995 Nov 15;312 ( Pt 1)(Pt 1):1-11.
- (45) Clapham DE. Calcium signaling. *Cell* 1995 Jan 27;80(2):259-268.
- (46) Huser J, Holda JR, Kockskamper J, Blatter LA. Focal agonist stimulation results in spatially restricted Ca<sup>2+</sup> release and capacitative Ca<sup>2+</sup> entry in bovine vascular endothelial cells. *J Physiol* 1999 Jan 1;514 ( Pt 1)(Pt 1):101-109.
- (47) Sedova M, Blatter LA. Dynamic regulation of [Ca<sup>2+</sup>]<sub>i</sub> by plasma membrane Ca(2+)-ATPase and Na<sup>+</sup>/Ca<sup>2+</sup> exchange during capacitative Ca<sup>2+</sup> entry in bovine vascular endothelial cells. *Cell Calcium* 1999 May;25(5):333-343.
- (48) Blatter LA, Taha Z, Mesaros S, Shacklock PS, Wier WG, Malinski T. Simultaneous measurements of Ca<sup>2+</sup> and nitric oxide in bradykinin-stimulated vascular endothelial cells. *Circ Res* 1995 May;76(5):922-924.
- (49) Berridge MJ. Calcium signalling and cell proliferation. *Bioessays* 1995 Jun;17(6):491-500.
- (50) Birnbaumer L, Boulay G, Brown D, Jiang M, Dietrich A, Mikoshiba K, et al. Mechanism of capacitative Ca<sup>2+</sup> entry (CCE): interaction between IP<sub>3</sub> receptor

and TRP links the internal calcium storage compartment to plasma membrane CCE channels. *Recent Prog Horm Res* 2000;55:127-61; discussion 161-2.

(51) Ma HT, Patterson RL, van Rossum DB, Birnbaumer L, Mikoshiba K, Gill DL. Requirement of the inositol trisphosphate receptor for activation of store-operated Ca<sup>2+</sup> channels. *Science* 2000 Mar 3;287(5458):1647-1651.

(52) Malli R, Frieden M, Hunkova M, Trenker M, Graier WF. Ca<sup>2+</sup> refilling of the endoplasmic reticulum is largely preserved albeit reduced Ca<sup>2+</sup> entry in endothelial cells. *Cell Calcium* 2007 Jan;41(1):63-76.

(53) Breier G, Breviario F, Caveda L, Berthier R, Schnurch H, Gotsch U, et al. Molecular cloning and expression of murine vascular endothelial-cadherin in early stage development of cardiovascular system. *Blood* 1996 Jan 15;87(2):630-641.

(54) Dejana E. Endothelial adherens junctions: implications in the control of vascular permeability and angiogenesis. *J Clin Invest* 1996 Nov 1;98(9):1949-1953.

(55) Sadler JE. Biochemistry and genetics of von Willebrand factor. *Annu Rev Biochem* 1998;67:395-424.

(56) Grynkiewicz G, Poenie M, Tsien RY. A new generation of Ca<sup>2+</sup> indicators with greatly improved fluorescence properties. *J Biol Chem* 1985 Mar 25;260(6):3440-3450.

(57) DIBLE JH. Organisation and canalisation in arterial thrombosis. *J Pathol Bacteriol* 1958 Jan;75(1):1-7.

(58) Wakefield TW, Linn MJ, Henke PK, Kadell AM, Wilke CA, Wroblewski SK, et al. Neovascularization during venous thrombosis organization: a preliminary study. *J Vasc Surg* 1999 Nov;30(5):885-892.

(59) Sevitt S. Organic canalisation and vascularisation of deep vein thrombi studied with dyed-micropaque injected at necropsy. *J Pathol* 1970 Feb;100(2):Pi.

(60) Yang L, Du J, Hou J, Jiang H, Zou J. Platelet factor-4 and its p17-70 peptide inhibit myeloma proliferation and angiogenesis in vivo. *BMC Cancer* 2011 Jun 21;11:261. doi:10.1186/1471-2407-11-261.

(61) Angiolillo AL, Sgadari C, Taub DD, Liao F, Farber JM, Maheshwari S, et al. Human interferon-inducible protein 10 is a potent inhibitor of angiogenesis in vivo. *J Exp Med* 1995 Jul 1;182(1):155-162.

(62) Bodnar RJ, Yates CC, Rodgers ME, Du X, Wells A. IP-10 induces dissociation of newly formed blood vessels. *J Cell Sci* 2009 Jun 15;122(Pt 12):2064-2077.

- (63) Zeng Y, Sun HR, Yu C, Lai Y, Liu XJ, Wu J, et al. CXCR1 and CXCR2 are novel mechano-sensors mediating laminar shear stress-induced endothelial cell migration. *Cytokine* 2011 Jan;53(1):42-51.
- (64) Walenta KL, Bettink S, Bohm M, Friedrich EB. Differential chemokine receptor expression regulates functional specialization of endothelial progenitor cell subpopulations. *Basic Res Cardiol* 2011 Mar;106(2):299-305.
- (65) Kimura H, Okada O, Tanabe N, Tanaka Y, Terai M, Takiguchi Y, et al. Plasma monocyte chemoattractant protein-1 and pulmonary vascular resistance in chronic thromboembolic pulmonary hypertension. *Am J Respir Crit Care Med* 2001 Jul 15;164(2):319-324.
- (66) Watson C, Whittaker S, Smith N, Vora AJ, Dumonde DC, Brown KA. IL-6 acts on endothelial cells to preferentially increase their adherence for lymphocytes. *Clin Exp Immunol* 1996 Jul;105(1):112-119.
- (67) Langer F, Schramm R, Bauer M, Tscholl D, Kuniyama T, Schafers HJ. Cytokine response to pulmonary thromboendarterectomy. *Chest* 2004 Jul;126(1):135-141.
- (68) Maruna P, Kunstyr J, Plocova KM, Mlejnsky F, Hubacek J, Klein AA, et al. Predictors of infection after pulmonary endarterectomy for chronic thromboembolic pulmonary hypertension. *Eur J Cardiothorac Surg* 2010 Jul 6.
- (69) Li A, Dubey S, Varney ML, Dave BJ, Singh RK. IL-8 directly enhanced endothelial cell survival, proliferation, and matrix metalloproteinases production and regulated angiogenesis. *J Immunol* 2003 Mar 15;170(6):3369-3376.
- (70) McGuinness CL, Humphries J, Waltham M, Burnand KG, Collins M, Smith A. Recruitment of labelled monocytes by experimental venous thrombi. *Thromb Haemost* 2001 Jun;85(6):1018-1024.
- (71) Singh I, Burnand KG, Collins M, Luttun A, Collen D, Boelhouwer B, et al. Failure of thrombus to resolve in urokinase-type plasminogen activator gene-knockout mice: rescue by normal bone marrow-derived cells. *Circulation* 2003 Feb 18;107(6):869-875.
- (72) Sakao S, Hao H, Tanabe N, Kasahara Y, Kurosu K, Tatsumi K. Endothelial-like cells in chronic thromboembolic pulmonary hypertension: crosstalk with myofibroblast-like cells. *Respir Res* 2011 Aug 22;12:109. doi:10.1186/1465-9921-12-109.
- (73) Hosokawa K, Ishibashi-Ueda H, Kishi T, Nakanishi N, Kyotani S, Ogino H. Histopathological multiple recanalized lesion is critical element of outcome after pulmonary thromboendarterectomy. *Int Heart J* 2011;52(6):377-381.
- (74) Preissner KT. Anticoagulant potential of endothelial cell membrane components. *Haemostasis* 1988;18(4-6):271-300.

- (75) Rosenberg RD, Bauer KA, Marcum JA. Protease inhibitors of human plasma. Antithrombin-III. "The heparin-antithrombin system". *J Med* 1985;16(1-3):351-416.
- (76) Coomber BL, Gotlieb AI. In vitro endothelial wound repair. Interaction of cell migration and proliferation. *Arteriosclerosis* 1990 Mar-Apr;10(2):215-222.
- (77) Tiruppathi C, Minshall RD, Paria BC, Vogel SM, Malik AB. Role of Ca<sup>2+</sup> signaling in the regulation of endothelial permeability. *Vascul Pharmacol* 2002 Nov;39(4-5):173-185.
- (78) Lum H, Malik AB. Regulation of vascular endothelial barrier function. *Am J Physiol* 1994 Sep;267(3 Pt 1):L223-41.
- (79) Dudek SM, Garcia JG. Cytoskeletal regulation of pulmonary vascular permeability. *J Appl Physiol* 2001 Oct;91(4):1487-1500.
- (80) Tran PO, Hinman LE, Unger GM, Sammak PJ. A wound-induced [Ca<sup>2+</sup>]<sub>i</sub> increase and its transcriptional activation of immediate early genes is important in the regulation of motility. *Exp Cell Res* 1999 Feb 1;246(2):319-326.
- (81) Erdogan A, Schaefer CA, Schaefer M, Luedders DW, Stockhausen F, Abdallah Y, et al. Margatoxin inhibits VEGF-induced hyperpolarization, proliferation and nitric oxide production of human endothelial cells. *J Vasc Res* 2005 Sep-Oct;42(5):368-376.
- (82) Wang R, Sauve R, de Champlain J. Altered calcium homeostasis in tail artery endothelial cells from spontaneously hypertensive rats. *Am J Hypertens* 1995 Oct;8(10 Pt 1):1023-1030.
- (83) Yu Y, Fantozzi I, Remillard CV, Landsberg JW, Kunichika N, Platoshyn O, et al. Enhanced expression of transient receptor potential channels in idiopathic pulmonary arterial hypertension. *Proc Natl Acad Sci U S A* 2004 Sep 21;101(38):13861-13866.
- (84) Maruoka M, Sakao S, Kantake M, Tanabe N, Kasahara Y, Kurosu K, et al. Characterization of myofibroblasts in chronic thromboembolic pulmonary hypertension. *Int J Cardiol* 2011 Mar 14;doi:10.1016/j.ijcard.2011.02.037. In press.
- (85) Files JC, Malpass TW, Yee EK, Ritchie JL, Harker LA. Studies of human platelet alpha-granule release in vivo. *Blood* 1981 Sep;58(3):607-618.
- (86) Fukami MH, Holmsen H, Kowalska MA, Niewiarowski S. Platelet secretion. In: Colman RW, Hirsh J, Marder VJ, Clowes AW, George JN, editors., editor. *Hemostasis and Thrombosis: Basic Principles and Clinical Practice Philadelphia*: Lippincott Williams & Wilkins; 2001. p. 561-573.
- (87) Taub DD, Lloyd AR, Conlon K, Wang JM, Ortaldo JR, Harada A, et al. Recombinant human interferon-inducible protein 10 is a chemoattractant for human monocytes and T lymphocytes and promotes T cell adhesion to endothelial cells. *J Exp Med* 1993 Jun 1;177(6):1809-1814.

- (88) Luster AD, Greenberg SM, Leder P. The IP-10 chemokine binds to a specific cell surface heparan sulfate site shared with platelet factor 4 and inhibits endothelial cell proliferation. *J Exp Med* 1995 Jul 1;182(1):219-231.
- (89) Struyf S, Salogni L, Burdick MD, Vandercappellen J, Gouwy M, Noppen S, et al. Angiostatic and chemotactic activities of the CXC chemokine CXCL4L1 (platelet factor-4 variant) are mediated by CXCR3. *Blood* 2011 Jan 13;117(2):480-488.
- (90) Romagnani P, Annunziato F, Lasagni L, Lazzeri E, Beltrame C, Francalanci M, et al. Cell cycle-dependent expression of CXC chemokine receptor 3 by endothelial cells mediates angiostatic activity. *J Clin Invest* 2001 Jan;107(1):53-63.
- (91) Hou Y, Plett PA, Ingram DA, Rajashekhar G, Orschell CM, Yoder MC, et al. Endothelial-monocyte-activating polypeptide II induces migration of endothelial progenitor cells via the chemokine receptor CXCR3. *Exp Hematol* 2006 Aug;34(8):1125-1132.
- (92) Colvin RA, Campanella GS, Sun J, Luster AD. Intracellular domains of CXCR3 that mediate CXCL9, CXCL10, and CXCL11 function. *J Biol Chem* 2004 Jul 16;279(29):30219-30227.
- (93) Mueller A, Meiser A, McDonagh EM, Fox JM, Petit SJ, Xanthou G, et al. CXCL4-induced migration of activated T lymphocytes is mediated by the chemokine receptor CXCR3. *J Leukoc Biol* 2008 Apr;83(4):875-882.
- (94) van Weering HR, de Jong AP, de Haas AH, Biber KP, Boddeke HW. CCL21-induced calcium transients and proliferation in primary mouse astrocytes: CXCR3-dependent and independent responses. *Brain Behav Immun* 2010 Jul;24(5):768-775.
- (95) Carmeliet P. Mechanisms of angiogenesis and arteriogenesis. *Nat Med* 2000 Apr;6(4):389-395.
- (96) De S, Razorenova O, McCabe NP, O'Toole T, Qin J, Byzova TV. VEGF-integrin interplay controls tumor growth and vascularization. *Proc Natl Acad Sci U S A* 2005 May 24;102(21):7589-7594.
- (97) Hofer E, Schweighofer B. Signal transduction induced in endothelial cells by growth factor receptors involved in angiogenesis. *Thromb Haemost* 2007 Mar;97(3):355-363.
- (98) Davis GE, Senger DR. Endothelial extracellular matrix: biosynthesis, remodeling, and functions during vascular morphogenesis and neovessel stabilization. *Circ Res* 2005 Nov 25;97(11):1093-1107.
- (99) Paria BC, Vogel SM, Ahmmed GU, Alamgir S, Shroff J, Malik AB, et al. Tumor necrosis factor-alpha-induced TRPC1 expression amplifies store-operated Ca<sup>2+</sup> influx and endothelial permeability. *Am J Physiol Lung Cell Mol Physiol* 2004 Dec;287(6):L1303-13.

- (100) Ye SQ, Zhang LQ, Adyshev D, Usatyuk PV, Garcia AN, Lavoie TL, et al. Pre-B-cell-colony-enhancing factor is critically involved in thrombin-induced lung endothelial cell barrier dysregulation. *Microvasc Res* 2005 Nov;70(3):142-151.
- (101) Grant DS, Tashiro K, Segui-Real B, Yamada Y, Martin GR, Kleinman HK. Two different laminin domains mediate the differentiation of human endothelial cells into capillary-like structures in vitro. *Cell* 1989 Sep 8;58(5):933-943.
- (102) Angiolillo AL, Sgadari C, Tosato G. A role for the interferon-inducible protein 10 in inhibition of angiogenesis by interleukin-12. *Ann N Y Acad Sci* 1996 Oct 31;795:158-167.
- (103) Klingberg F, Hinz B, White ES. The myofibroblast matrix: implications for tissue repair and fibrosis. *J Pathol* 2012 Sep 21.
- (104) Streuli CH, Schmidhauser C, Kobrin M, Bissell MJ, Derynck R. Extracellular matrix regulates expression of the TGF-beta 1 gene. *J Cell Biol* 1993 Jan;120(1):253-260.
- (105) Hoh BL, Hosaka K, Downes DP, Nowicki KW, Fernandez CE, Batich CD, et al. Monocyte chemoattractant protein-1 promotes inflammatory vascular repair of murine carotid aneurysms via a macrophage inflammatory protein-1alpha and macrophage inflammatory protein-2-dependent pathway. *Circulation* 2011 Nov 15;124(20):2243-2252.
- (106) Tatewaki H, Egashira K, Kimura S, Nishida T, Morita S, Tominaga R. Blockade of monocyte chemoattractant protein-1 by adenoviral gene transfer inhibits experimental vein graft neointimal formation. *J Vasc Surg* 2007 Jun;45(6):1236-1243.
- (107) Saiura A, Sata M, Hiasa K, Kitamoto S, Washida M, Egashira K, et al. Antimonocyte chemoattractant protein-1 gene therapy attenuates graft vasculopathy. *Arterioscler Thromb Vasc Biol* 2004 Oct;24(10):1886-1890.
- (108) Mori E, Komori K, Yamaoka T, Tanii M, Kataoka C, Takeshita A, et al. Essential role of monocyte chemoattractant protein-1 in development of restenotic changes (neointimal hyperplasia and constrictive remodeling) after balloon angioplasty in hypercholesterolemic rabbits. *Circulation* 2002 Jun 18;105(24):2905-2910.
- (109) Egashira K, Zhao Q, Kataoka C, Ohtani K, Usui M, Charo IF, et al. Importance of monocyte chemoattractant protein-1 pathway in neointimal hyperplasia after periarterial injury in mice and monkeys. *Circ Res* 2002 Jun 14;90(11):1167-1172.
- (110) Furukawa Y, Matsumori A, Ohashi N, Shioi T, Ono K, Harada A, et al. Anti-monocyte chemoattractant protein-1/monocyte chemoattractant and activating factor antibody inhibits neointimal hyperplasia in injured rat carotid arteries. *Circ Res* 1999 Feb 19;84(3):306-314.

(111) Liehn EA, Piccinini AM, Koenen RR, Soehnlein O, Adage T, Fatu R, et al. A new monocyte chemotactic protein-1/chemokine CC motif ligand-2 competitor limiting neointima formation and myocardial ischemia/reperfusion injury in mice. *J Am Coll Cardiol* 2010 Nov 23;56(22):1847-1857.

(112) Morimoto H, Takahashi M, Izawa A, Ise H, Hongo M, Kolattukudy PE, et al. Cardiac overexpression of monocyte chemoattractant protein-1 in transgenic mice prevents cardiac dysfunction and remodeling after myocardial infarction. *Circ Res* 2006 Oct 13;99(8):891-899.

(113) Gharaee-Kermani M, Denholm EM, Phan SH. Costimulation of fibroblast collagen and transforming growth factor beta1 gene expression by monocyte chemoattractant protein-1 via specific receptors. *J Biol Chem* 1996 Jul 26;271(30):17779-17784.

(114) Koch AE, Polverini PJ, Kunkel SL, Harlow LA, DiPietro LA, Elner VM, et al. Interleukin-8 as a macrophage-derived mediator of angiogenesis. *Science* 1992 Dec 11;258(5089):1798-1801.

(115) Schraufstatter IU, Chung J, Burger M. IL-8 activates endothelial cell CXCR1 and CXCR2 through Rho and Rac signaling pathways. *Am J Physiol Lung Cell Mol Physiol* 2001 Jun;280(6):L1094-103.

(116) McCawley LJ, Matrisian LM. Matrix metalloproteinases: multifunctional contributors to tumor progression. *Mol Med Today* 2000 Apr;6(4):149-156.

(117) Soon E, Holmes AM, Barker L, Treaty C, Suntharalingham J, Toshner M, et al. Inflammatory Cytokines are Elevated in Patients with Operable Chronic Thromboembolic Pulmonary Hypertension and Predict Outcome Post-Endarterectomy. *Thorax* 2010 DEC;65:A45-A45.

## **Acknowledgement**

This PhD thesis is the result of work and study at the center of medical research (ZMF) in the Department of Anaesthesiology and Intensive Care at the Medical University of Graz as well as the Ludwig Boltzmann Institute for Lung Vascular Research. During this time I had the support of many people I wish to acknowledge now.

First of all I would like to thank my supervisor Prof. Andrea Olschewski, who was inspiring and supporting me.

Secondly I would like to express my deepest gratitude to Dr. Zoltán Bálint, who introduced me to the world of live cell calcium imaging. Under his guidance I learned to develop my experimental skills and the way of thinking about scientific questions. I am thankful for the time he offered me when I had questions or needed his advice, which broadened my knowledge and made my work and life easier. Special thanks also go to Horst Olschewski, Chandran Nagarai, Akos Heinemann and Elvira Stacher who gave me scientific advice throughout my PhD thesis. Additionally I would like to thank Sabine Halsegger, Eva-Maria Schwarzl, Elisabeth Pöllitzer and Martina Ofner for their excellent technical support. I am also grateful for the cooperation with Prof. Walter Klepetko, Patrick Nierlich, Prof. Irene Lang and Prof. Shahrokh Taghavi from the Medical University of Vienna, who gave me access to PEA material and of course I would like to thank the patients and donors who made the whole study possible by offering me PEA and blood samples.

Special thanks go to my parents and my sister for their support, love and their patience with me. A big “thank you” to all my friends, who accompanied me during this period and made my life amusing and enjoyable.